

Fast-slow systems with codimension 2 fold points

Department of Applied Mathematics and Physics
Kyoto University, Kyoto, 606-8501, Japan
Hayato CHIBA ^{*1}

July 31 2008; Revised Sep 12, 2008

Abstract

The existence of stable periodic orbits and chaotic invariant sets of singularly perturbed problems of fast-slow type with codimension two fold points is proved by means of the boundary layer technique and the blow-up method. In particular, the blow-up method is effectively used for analyzing the flow near the fold points in order to show that slow manifolds near the codimension two fold points are extended along a solution of a perturbed first Painlevé equation in the blow-up space.

1 Introduction

Let $(x_1, \dots, x_n, y_1, \dots, y_m) \in \mathbf{R}^{n+m}$ be the Cartesian coordinates. Singularly perturbed ordinary differential equations of the form

$$\begin{cases} \dot{x}_1 = f_1(x_1, \dots, x_n, y_1, \dots, y_m, \varepsilon), \\ \vdots \\ \dot{x}_n = f_n(x_1, \dots, x_n, y_1, \dots, y_m, \varepsilon), \\ \dot{y}_1 = \varepsilon g_1(x_1, \dots, x_n, y_1, \dots, y_m, \varepsilon), \\ \vdots \\ \dot{y}_m = \varepsilon g_m(x_1, \dots, x_n, y_1, \dots, y_m, \varepsilon), \end{cases} \quad (1.1)$$

^{*1} E mail address : chiba@amp.i.kyoto-u.ac.jp

are called a *fast-slow system*, where the dot ($\dot{\cdot}$) denotes the derivative with respect to time t , and where $\varepsilon > 0$ is a small parameter. The unperturbed system of this system is given by

$$\begin{cases} \dot{x}_1 = f_1(x_1, \dots, x_n, y_1, \dots, y_m, 0), \\ \vdots \\ \dot{x}_n = f_n(x_1, \dots, x_n, y_1, \dots, y_m, 0), \\ \dot{y}_1 = 0, \\ \vdots \\ \dot{y}_m = 0. \end{cases} \quad (1.2)$$

The set of fixed points of the unperturbed system is called a *critical manifold*, which is defined by

$$\mathcal{M} = \{(x_1, \dots, x_n, y_1, \dots, y_m) \in \mathbf{R}^{n+m} \mid f_i(x_1, \dots, x_n, y_1, \dots, y_m, 0) = 0, i = 1, \dots, n\}. \quad (1.3)$$

Typically \mathcal{M} is an m -dimensional manifold. Fenichel [6] proved that if \mathcal{M} is normally hyperbolic, then the original system (1.1) with sufficiently small $\varepsilon > 0$ has a locally invariant manifold $\tilde{\mathcal{M}}$ near \mathcal{M} , and that dynamics on $\tilde{\mathcal{M}}$ is approximately given by the m -dimensional *slow system*

$$\begin{cases} \dot{y}_1 = \varepsilon g_1(x_1, \dots, x_n, y_1, \dots, y_m, \varepsilon), \\ \vdots \\ \dot{y}_m = \varepsilon g_m(x_1, \dots, x_n, y_1, \dots, y_m, \varepsilon), \end{cases} \quad (1.4)$$

where $(x_1, \dots, x_n, y_1, \dots, y_m) \in \mathbf{R}^{n+m}$ is restricted to the critical manifold \mathcal{M} . The $\tilde{\mathcal{M}}$ is diffeomorphic to \mathcal{M} and called the *slow manifold*. His method for constructing an approximate flow on the slow manifold is called the *geometric singular perturbation method*.

However, if the critical manifold \mathcal{M} has degenerate points $\mathbf{x}_0 \in \mathcal{M}$ in the sense that the Jacobian matrix $\partial \mathbf{f} / \partial \mathbf{x}$, $\mathbf{f} = (f_1, \dots, f_n)$, $\mathbf{x} = (x_1, \dots, x_n)$ at \mathbf{x}_0 has eigenvalues on the imaginary axis, then \mathcal{M} is not normally hyperbolic near the \mathbf{x}_0 and Fenichel's theory is no longer applicable. The most common case is that $\partial \mathbf{f} / \partial \mathbf{x}$ has one zero eigenvalue at \mathbf{x}_0 and the critical manifold \mathcal{M} is folded at the point (*fold point*). In this case, orbits on the slow manifold $\tilde{\mathcal{M}}$ may jump and get away from $\tilde{\mathcal{M}}$ in the vicinity of \mathbf{x}_0 . As a result, global phenomena such as a relaxation oscillation may occur. See Mischenko and Rozov [13], Jones [10], and references therein for treatments of jump points and the existence of relaxation oscillations based on the boundary layer technique and the geometric singular perturbation method.

The blow-up method was developed by Dumortier [4] to investigate local flows near non-hyperbolic fixed points and it was applied to singular perturbed problems by Dumortier and

Roussarie [5]. Analysis near fold points based on the blow-up method was extended to more general situations by Krupa and Szmolyan [11] in the case of $n = m = 1$ and by Szmolyan and Wechselberger [17] in the case of $n = 1, m = 2$. See also [7,8,12].

If the Jacobian matrix $\partial f/\partial \mathbf{x}$ at a fold point \mathbf{x}_0 has exactly k zero eigenvalues and other eigenvalues do not lie on the imaginary axis, then we call \mathbf{x}_0 the *codimension k fold point*. Codimension 1 fold points are studied in [7,8,11,12,13]. It is to be noted that the classical work of Mischenko and Rozov [13] is essentially equivalent to the blow-up method and it is shown therein that for *any* n and m , the flow of a fast-slow system near a codimension 1 fold point is reduced to a perturbed Riccati equation in the blow-up space.

However, despite many works, behavior near codimension k fold points with $k \geq 2$ is not understood well. One of the purposes of this article is to investigate codimension 2 fold points of the 3-dimensional fast-slow system of the form

$$\begin{cases} \dot{x} = f_1(x, y, z, \varepsilon, \delta), \\ \dot{y} = f_2(x, y, z, \varepsilon, \delta), \\ \dot{z} = \varepsilon g(x, y, z, \varepsilon, \delta), \end{cases} \quad (1.5)$$

where f_1, f_2, g are C^∞ functions, $\varepsilon > 0$ is a small parameter, and where $\delta \in \mathbf{R}$ is a parameter whose role will be explained later in detail (see the assumption (A5) in Sec.2). Note that the critical manifold

$$\mathcal{M} = \{(x, y, z) \in \mathbf{R}^3 \mid f_1(x, y, z, 0, \delta) = f_2(x, y, z, 0, \delta) = 0\} \quad (1.6)$$

gives curves on \mathbf{R}^3 in general. For this system, we will show that a perturbed first Painlevé equation plays an important role in the analysis of codimension 2 fold points. This is in contrast with the fact that the Riccati equation appears in the case of codimension 1 fold points. We also investigate global behavior of the system. Under some assumptions, we will prove that there exists a stable periodic orbit if $\varepsilon > 0$ is sufficiently small for fixed δ , and further that there exists a chaotic invariant set if $\delta > 0$ is also small in comparison with small ε .

While chaotic attractors on 3-dimensional fast-slow systems are reported by Guckenheimer, Wechselberger and Young [8] in the case of $n = 1, m = 2$, our system is of $n = 2, m = 1$. In the situation of [8], the chaotic attractor arises according to the theory of Hénon-like maps. On the other hand, in our system, the mechanism for the existence of chaotic invariant sets is quite similar to that in Silnikov's work [16], in which the existence of a denumerable set of periodic orbits is shown for a 3-dimensional system which have a

fixed point of saddle-focus type with a homoclinic orbit. See also Wiggins [18]. Indeed, in our situation, the critical manifold \mathcal{M} plays a similar role to the fixed point of saddle-focus type in the Silnikov's system. Our chaotic invariant sets seem to be attracting as that in [8], however, it remains unsolved. See Homburg [20] for the proof of the existence of chaotic attractors in the Silnikov's system.

This paper is organized as follows. In section 2, we give statements of our theorems on the existence of a periodic orbit and a chaotic invariant set. An intuitive explanation of the theorems is also shown with an example. In section 3, local analysis near the codimension 2 fold points is given by means of the blow-up method. Section 4 is devoted to global analysis, and proofs of Thms.1 and 2 are given. Concluding remarks are included in section 5.

2 Main theorems

We consider the system (1.5) with C^∞ functions f_1, f_2, g and parameters $\varepsilon > 0$ and $\delta \in \mathbf{R}$. The unperturbed system of Eq.(1.5) is given by

$$\begin{cases} \dot{x} = f_1(x, y, z, 0, \delta), \\ \dot{y} = f_2(x, y, z, 0, \delta), \\ \dot{z} = 0. \end{cases} \quad (2.1)$$

Since z is a constant, this system is regarded as a family of 2-dimensional systems. To show the existence of a stable periodic orbit, we make the following assumptions (A1) to (A4).

(A1) The critical manifold \mathcal{M} has two ‘‘J-shaped’’ components $S^+ = S_a^+ \cup \{L^+\} \cup S_r^+$ and $S^- = S_a^- \cup \{L^-\} \cup S_r^-$, where S_a^\pm consist of stable focus type fixed points, S_r^\pm consist of saddle type fixed points, and where L^\pm are codimension 2 fold points (see Fig.1).

(A2) The L^\pm are nondegenerate bifurcation points of Eq.(2.1) in the sense that normal forms of Eq.(2.1) near the points L^\pm are in the generic case. In particular, Eq.(2.1) has cusps at L^\pm .

(A3) Eq.(2.1) has two heteroclinic orbits α^+ and α^- which connect L^+, L^- with points on S_a^-, S_a^+ , respectively.

(A4) The function $g(x, y, z, 0, \delta)$ is negative and positive in the vicinity of $S_a^+ \cup \{L^+\}$ and of $S_a^- \cup \{L^-\}$, respectively.

A few remarks are in order. The S^+ and S^- are allowed to be connected. In this case, $S^+ \cup S^-$ is typically of ‘‘S-shaped’’. The fact that L^\pm are the codimension 2 fold points results from the assumptions for S_a^\pm and S_r^\pm . Indeed, since S_r^\pm and S_a^\pm are saddles and focuses,

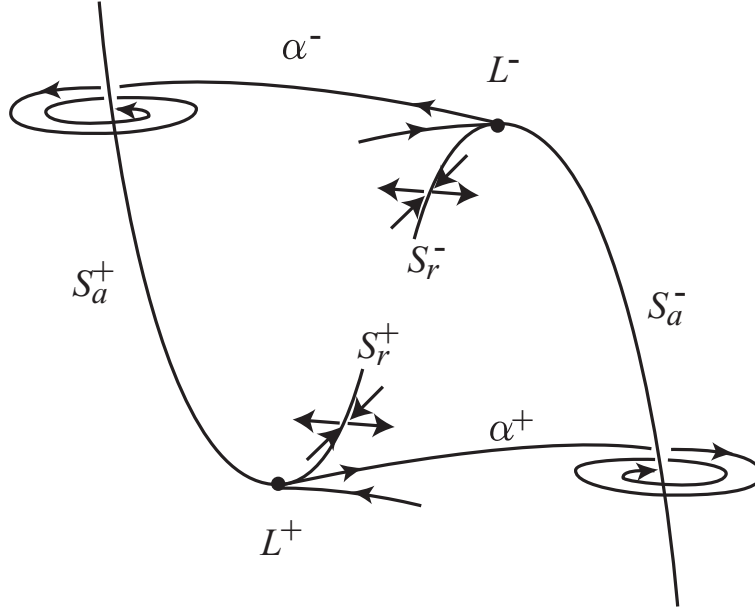


Fig. 1 Critical manifold and the flow of Eq.(2.1).

respectively, the Jacobian matrix $\partial(f_1, f_2)/\partial(x, y)$ has two zero eigenvalues at L^\pm (i.e. L^\pm are codimension 2 bifurcation points). Thus there exists a coordinate transformation $(x, y) \mapsto (X, Y)$ defined near L^+ such that L^+ is placed at the origin and Eq.(2.1) takes the following normal form

$$\begin{cases} \dot{X} = a_1 + a_2 Y^2 + a_3 XY + O(X^3, X^2 Y, XY^2, Y^3), \\ \dot{Y} = b_1 + b_2 X + O(X^3, X^2 Y, XY^2, Y^3), \\ \dot{z} = 0, \end{cases} \quad (2.2)$$

where a_1, a_2, a_3, b_1, b_2 are constants depending on z, ε, δ (for the normal form theory, see Chow, Li and Wang [3]). Then the assumption (A2) means that $a_2 \neq 0, a_3 \neq 0, b_2 \neq 0$ at L^+ . In this case, it is well known that the flow of Eq.(2.2) has a cusp at the origin, which corresponds to L^+ (see also Lemma 3.1). The normal form of Eq.(2.1) near L^- takes the same form. Since L^\pm are cusps, there exist exactly two orbits of Eq.(2.1) which converges to L^+, L^- as $t \rightarrow -\infty$, respectively. They are the heteroclinic orbits α^\pm assumed in (A3).

Under these assumptions, we can prove the next theorem.

Theorem.1 Suppose that assumptions (A1) to (A4) hold for a fixed $\delta \in \mathbf{R}$. Then there exists a positive number $\varepsilon_0 = \varepsilon_0(\delta)$ such that Eq.(1.5) has a stable periodic orbit near $S_a^+ \cup \alpha^+ \cup S_a^- \cup \alpha^-$ if $0 < \varepsilon < \varepsilon_0$.

To show the existence of a chaotic invariant set, we need additional assumptions (A5) and (A6).

(A5) Eigenvalues of the Jacobian matrix $\partial(f_1, f_2)/\partial(x, y)$ of Eq.(2.1) at $(x, y, z) \in S_a^+$ and at $(x, y, z) \in S_a^-$ are expressed by $-\delta\mu^+(z, \delta) \pm \sqrt{-1}\omega^+(z, \delta)$ and $-\delta\mu^-(z, \delta) \pm \sqrt{-1}\omega^-(z, \delta)$, respectively, where μ^\pm and ω^\pm are real-valued functions satisfying

$$\mu^\pm(z, 0) > 0, \quad \omega^\pm(z, 0) \neq 0. \quad (2.3)$$

The assumption (A5) means that the parameter δ controls the strength of stability of stable focus fixed points on S_a^\pm .

Let z_0^+ and z_0^- be z components of the coordinates of the fold points L^+ and L^- , respectively. Because of the assumption (A5), there exist open neighborhoods V^+, V^- of points $\alpha^- \cap S_a^+, \alpha^+ \cap S_a^-$ such that solutions of the system

$$\dot{x} = f_1(x, y, z_0^\pm, 0, \delta), \quad \dot{y} = f_2(x, y, z_0^\pm, 0, \delta), \quad (2.4)$$

whose initial values are on V^\pm , converge to the points $\alpha^- \cap S_a^+, \alpha^+ \cap S_a^-$ with the exponential rates $O(\exp[-\delta\mu^\pm(z_0^\pm, \delta)t])$, respectively. In general, the ‘‘radii’’ of V^\pm depend on δ and they may tend to zero as $\delta \rightarrow 0$. To prove Theorem 2 below, we assume that

(A6) The V^\pm with the above property are taken so that they are independent of δ .

A way to verify (A6) will be shown below along with an example.

Theorem 2. Suppose that there exists a positive number δ_0 such that the assumptions (A1) to (A6) hold for $0 < \delta < \delta_0$. Then, there exist a positive number ε_0 and positive valued functions $\delta_1(\varepsilon), \delta_2(\varepsilon)$ such that if $0 < \varepsilon < \varepsilon_0$ and $\delta_1(\varepsilon) < \delta < \delta_2(\varepsilon)$, then Eq.(1.5) has a hyperbolic horseshoe near $S_a^+ \cup \alpha^+ \cup S_a^- \cup \alpha^-$.

Theorems 1 and 2 mean that if $\varepsilon > 0$ is sufficiently small for a fixed δ , then there exists a stable periodic orbit. However, as δ decreases, the periodic orbit undergoes a succession of bifurcations and if δ gets sufficiently small in comparison with ε , then a chaotic invariant set appears. We conjecture that this chaotic invariant set is attracting.

In the rest of this section, we give an intuitive explanation of the theorems with an example.

Consider the system

$$\begin{cases} \dot{x} = z + 3(y^3 - y) + \delta x \left(\frac{1}{3} - y^2 \right), \\ \dot{y} = -x, \\ \dot{z} = \varepsilon \sin\left(\frac{5}{2}y\right). \end{cases} \quad (2.5)$$

The critical manifold \mathcal{M} is given by the curve $z = 3(y - y^3)$, $x = 0$, and the fold points are given by $L^\pm = (0, \mp \frac{1}{\sqrt{3}}, \mp \frac{2}{\sqrt{3}})$, see Fig. 2.

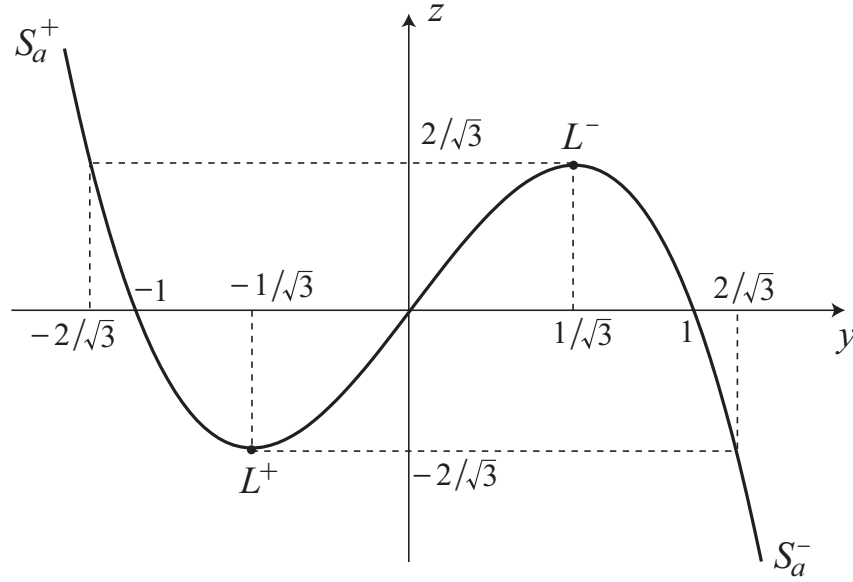


Fig. 2 Critical manifold of the system (2.5).

It is easy to verify that the assumptions (A1), (A2), (A4) and (A5) are satisfied for (2.5). The assumption (A3) of existence of heteroclinic orbits are verified numerically (we do not give a proof here).

To verify the assumption (A6), we change the coordinates by an affine transformation $(x, y, z) \mapsto (X, Y, Z)$ so that the point $\alpha^- \cap S_a^+ = (0, -2/\sqrt{3}, 2/\sqrt{3})$ is placed at the origin and the linear part of Eq.(2.5) is diagonalized. Then the unperturbed system of Eq.(2.5) is rewritten as

$$\frac{d}{dt} \begin{pmatrix} X \\ Y \end{pmatrix} = \frac{\sqrt{-1}}{2} \sqrt{36 - \delta^2} \begin{pmatrix} -1 & 0 \\ 0 & 1 \end{pmatrix} \begin{pmatrix} X \\ Y \end{pmatrix} - \frac{\delta}{2} \begin{pmatrix} 1 & 0 \\ 0 & 1 \end{pmatrix} \begin{pmatrix} X \\ Y \end{pmatrix} + h(X, Y, \delta), \quad (2.6)$$

where the explicit form of the polynomial h , whose degree is greater than one, is too compli-

cated to be written here. However, one can verify that h is of the form

$$h(X, Y, \delta) = \sqrt{-1}h_1(X, Y, \delta) + \delta h_2(X, Y, \delta), \quad (2.7)$$

where h_1 and h_2 are polynomials with respect to X and Y such that all coefficients of h_1 are real. Note that Eq.(2.6) corresponds to Eq.(2.4) along with $\sqrt{36 - \delta^2}/2$ and $\delta/2$ corresponding to $\omega^+(z_0^+, \delta)$ and $\delta\mu^+(z_0^+, \delta)$, respectively, in the assumption (A5).

Now we bring Eq.(2.6) into the normal form with respect to the first term of the right hand side. There exist a neighborhood W of the origin, which is independent of δ , and a coordinate transformation $(X, Y) \mapsto (r, \theta)$ defined on W such that Eq.(2.6) is put in the form

$$\begin{cases} \dot{r} = -\frac{\delta}{2}r + a_3r^3 + a_5r^5 + \dots, \\ \dot{\theta} = \sqrt{36 - \delta^2}/2 + O(r^2). \end{cases} \quad (2.8)$$

Note that the equation of the radius r is independent of θ (see Chow, Li and Wang [3]). In our case, a_3 is given by

$$a_3 = \delta \frac{-180 + 29\delta^2}{6(36 - \delta^2)^2}. \quad (2.9)$$

Further, we can prove that $a_i \sim O(\delta)$, $i = 3, 5, \dots$ as $\delta \rightarrow 0$ by using the induction together with the property that $h(X, Y, 0)$ takes purely imaginary values if $(X, Y) \in \mathbf{R}^2$ (see Eq.(2.7)). See the appendix of Chiba [2] for explicit formulas of the normal form which are convenient for the induction. Thus the derivative of the right hand side of Eq.(2.8) is calculated as

$$\frac{d}{dr} \left(-\frac{\delta}{2}r + a_3r^3 + \dots \right) = -\frac{\delta}{2}(1 + b_3r^2 + b_5r^4 + \dots) + O(\delta^2), \quad (2.10)$$

where b_3, b_5, \dots are δ -independent constants. It proves that there exists a δ -independent positive constant C such that if $|r(0)| < C$, then $r(t)$ decays as $|r(t)| \sim O(e^{-\delta t/2})$ for small $\delta > 0$. This verifies the assumption (A6).

Figure 3 shows numerical results for Eq.(2.5). If $\varepsilon = 0.02$ and $\delta = 0.06$, there exists a stable periodic orbit (Fig.3 (a)) while a chaotic behavior occurs if $\varepsilon = 0.02$ and $\delta = 0.03$ (Fig.3 (b)). This verifies Theorems 1 and 2 for Eq.(2.5).

Although Theorem 2 does not state that chaotic invariant sets mentioned are attracting, Figure 3 (c) corroborates numerically that the chaotic invariant set for our example is actually a chaotic attractor. Take the Poincaré section $\Sigma_1 = \{(x, y, z) | y = 0.5, z > 0\}$ and $\Sigma_2 = \{(x, y, z) | y = -0.5, z < 0\}$, like as Σ_{out}^- and Σ_{out}^+ in Fig.4, respectively. Since Eq.(2.5) admits the symmetry $(x, y, z) \mapsto (-x, -y, -z)$ and Σ_1 corresponds to Σ_2 under the symmetry,

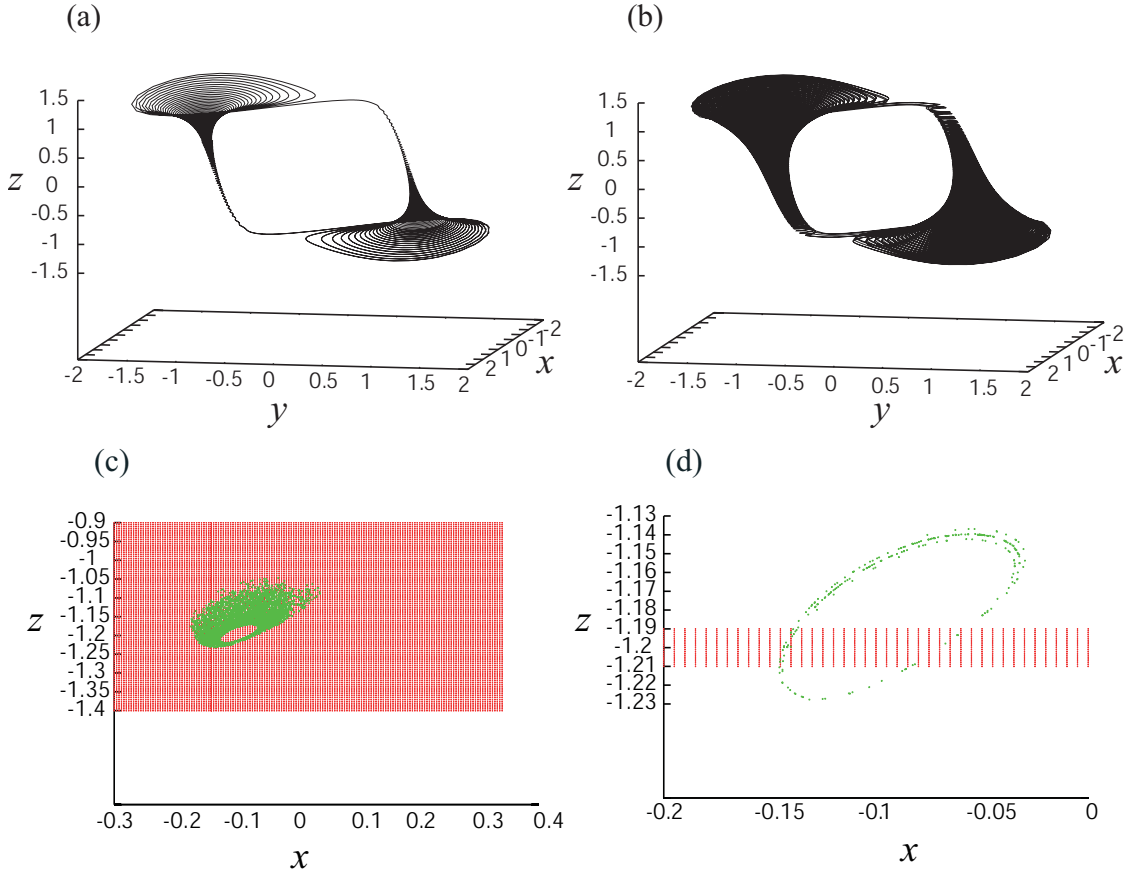


Fig. 3 Numerical results for Eq.(2.5). If (a) $\varepsilon = 0.02$ and $\delta = 0.06$, there exists a stable periodic orbit and if (b) $\varepsilon = 0.02$ and $\delta = 0.03$, there exists a chaotic attractor. In (c) and (d), the green points denote the image of the red points under the Poincaré map from Σ_1 to Σ_2 . They show that the Poincaré map has a horseshoe and it is attracting.

we identify them and calculate the Poincaré map from Σ_1 to Σ_2 . The results are represented in Fig.3 (c) and (d). The red points on Σ_1 , identified with Σ_2 , are mapped to the green points on Σ_2 by the Poincaré map. Fig.3(c) and (d) show that the Poincaré map is attracting and it has a horseshoe, respectively.

To ascertain the reason why the periodic orbit or the chaotic attractor occur, we take Poincaré sections Σ_{out}^+ , Σ_{II}^- , Σ_{in}^- , Σ_{out}^- , Σ_{II}^+ and Σ_{in}^+ as in Fig. 4.

The section Σ_{out}^+ is parallel to the xz plane and located at the right of L^+ . Take a rectangle R on Σ_{out}^+ and consider how it behaves when it runs along solutions of Eq.(2.5). Since the unperturbed system of Eq.(2.5) has the heteroclinic orbit α^+ connecting L^+ and S_a^- , the rectangle R

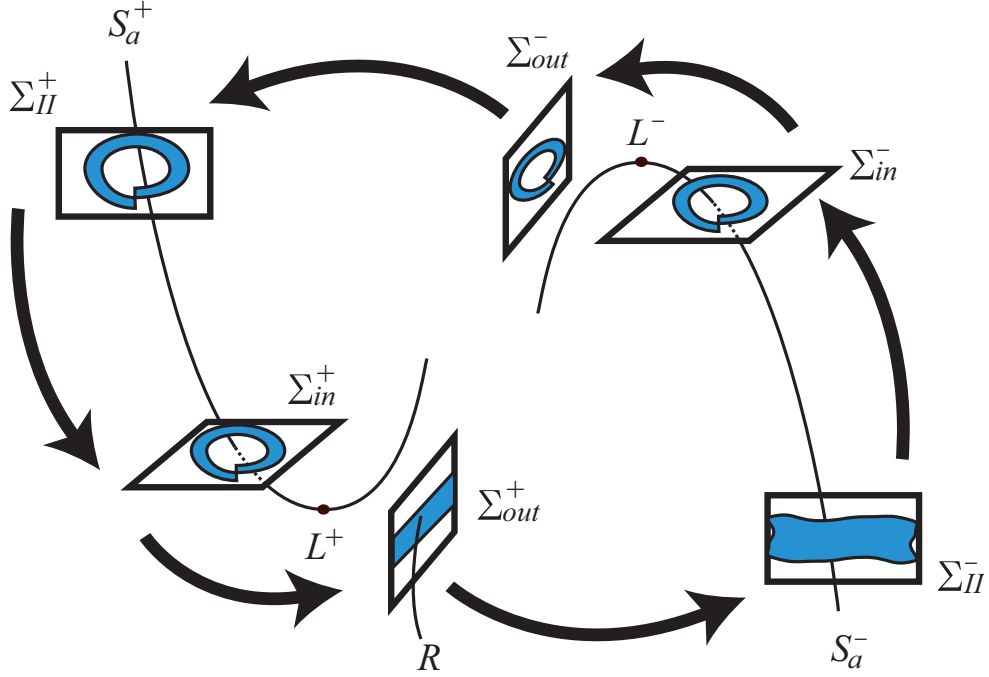


Fig. 4 Poincaré sections and a schematic view of the images of the rectangle R under a succession of the transition maps.

also approaches to S_a^- along α^+ and intersects the section Σ_{II}^- , as is shown in Fig. 4. Since the velocity $\varepsilon \sin(5y/2)$ in the direction z is positive in the vicinity of S_a^- and since S_a^- consists of stable focus fixed points, the intersection area on Σ_{II}^- moves upward, rotating around S_a^- . As a result, the flow of R intersects the section Σ_{in}^- , which is parallel to the xy plane, to form a ring-shaped area as is shown in Figure 4. Further, we can show that the ring-shaped area on Σ_{in}^- moves to Σ_{out}^- along solutions of Eq.(2.5) by using the blow-up method, as is proved in Sec.3. The area on Σ_{out}^- goes back to the section Σ_{out}^+ in a similar manner because Eq.(2.5) has the symmetry $(x, y, z) \mapsto (-x, -y, -z)$. Thus the Poincaré return map Π from Σ_{out}^+ into itself is well-defined and it turns out that $\Pi(R)$ is ring-shaped.

There are two possibilities of locations of the returned ring-shaped area. If the strength of stability of stable fixed points on S_a^\pm , say δ as in the assumption (A5), is sufficiently large, then the radius of the ring-shaped area gets sufficiently small when passing around S_a^\pm . As a result, the returned ring-shaped area is included in the rectangle R as in Fig.5 (a). It means that the Poincaré map Π is contractive and it has a stable fixed point, which corresponds to a stable periodic orbit of Eq.(2.5). On the other hand, if the strength δ is not so large, the radius

of the ring-shaped area is not so small and it intersects with the rectangle as in Fig.5 (b). In this case, the Poincaré map Π has a horseshoe. Actually we will prove that this horseshoe is hyperbolic in Sec.4.

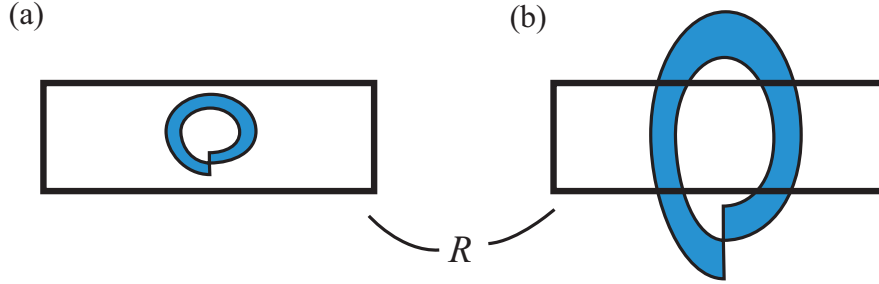


Fig. 5 Positional relationship of the rectangle R with the returned ring-shaped area.

3 Local analysis around the fold points

In this section, we give a local analysis around the fold points L^\pm by using the blow-up method and calculate a transition map to observe how orbits of Eq.(1.5) behave near the fold points. The main theorem in this section (Thm.3.2) will be made in the end of Sec.3.1. We will calculate only for L^+ because discussion for L^- is done in the same way.

3.1 Normal form coordinates

At first, we transform Eq.(1.5) into the normal form in the vicinity of L^+ . In what follows, if a (formal) power series h centered at the origin begins with n -th degree terms (*i.e.* $\partial^i h(0)/\partial \mathbf{x}^i = 0$ ($i = 0, 1, \dots, n-1$) and $\partial^n h(0)/\partial \mathbf{x}^n \neq 0$), we denote the fact as $h \sim O_p(n)$. The notation $O(\cdot)$ is used to the usual Landau notation.

Lemma 3.1. There exists a local coordinate transformation $(x, y, z) \mapsto (X, Y, Z)$ defined near L^+ such that Eq.(1.5) is brought into the form

$$\begin{cases} \dot{X} = Z - Y^2 + c_1 XY + c_2 \varepsilon + Zh_1(X, Y, Z) + Y^2 h_2(X, Y, Z) + \varepsilon h_3(X, Y, Z, \varepsilon), \\ \dot{Y} = -X + c_3 \varepsilon + Zh_4(X, Y, Z) + \varepsilon h_5(X, Y, Z, \varepsilon), \\ \dot{Z} = -\varepsilon + \varepsilon h_6(X, Y, Z, \varepsilon), \end{cases} \quad (3.1)$$

where $c_1 > 0$, c_2, c_3 are constants and $h_i \sim O_p(1)$ ($i = 1, \dots, 6$) are C^∞ functions all of which may depend on δ (in this section, the parameter δ does not play a role and we omit to mention

it).

In these coordinates, L^+ is placed at the origin and the branch S^+ of the critical manifold is of the form $Z = Y^2 + O_p(3)$, $X = O_p(2)$.

Proof of the Lemma. We start by calculating the normal form of the unperturbed system (2.1). We will use the same notation (x, y, z) as the original coordinates after a succession of coordinate transformations for simplicity. Since the Jacobian matrix of (f_1, f_2) at L^+ has two zero eigenvalues due to the assumption (A1), the normal form for the equations of (x, y) is of the form (see Chow, Li and Wang [3])

$$\begin{cases} \dot{x} = a_1 z + a_2 y^2 + a_3 xy + zh_1(x, y, z) + y^2 h_2(x, y, z), \\ \dot{y} = b_1 x + b_2 z + zh_4(x, y, z), \end{cases} \quad (3.2)$$

where a_1, a_2, a_3, b_1, b_2 are constants and $h_1, h_2, h_4 \sim O_p(1)$ are C^∞ functions. Note that $a_2 \neq 0, a_3 \neq 0, b_1 \neq 0$ because of the assumption (A2). Since we can assume that S^+ is locally expressed as $y = z^2, x = 0$ without loss of generality, we obtain $a_2 = -a_1$ and $b_2 = 0$. Since fixed points on S_a^+ are attracting and since fixed points on S_r^+ are saddles, we obtain $a_1 b_1 < 0$ and $a_3 > 0$. We can assume that $a_1 > 0$ because we are allowed to change the coordinates as $x \mapsto -x$ if necessary. Thus, the normal form of Eq.(2.1) is written as

$$\begin{cases} \dot{x} = a_1(z - y^2) + a_3 xy + zh_1(x, y, z) + y^2 h_2(x, y, z), \\ \dot{y} = b_1 x + zh_4(x, y, z), \\ \dot{z} = 0, \end{cases} \quad (3.3)$$

with $a_1 > 0, a_3 > 0, b_1 < 0$. The coordinate transformation which brings Eq.(2.1) into Eq.(3.3) transforms Eq.(1.5) into the system of the form

$$\begin{cases} \dot{x} = a_1(z - y^2) + a_3 xy + zh_1(x, y, z) + y^2 h_2(x, y, z) + a_4 \varepsilon + \varepsilon h_3(x, y, z, \varepsilon), \\ \dot{y} = b_1 x + zh_4(x, y, z) + b_3 \varepsilon + \varepsilon h_5(x, y, z, \varepsilon), \\ \dot{z} = \varepsilon(g_1 + h_6(x, y, z, \varepsilon)), \end{cases} \quad (3.4)$$

where a_4, b_3 are constants, $h_3, h_5, h_6 \sim O_p(1)$ are C^∞ functions, and where $g_1 := g(L^+, 0, \delta)$ is a negative constant on account of the assumption (A4). Finally, changing coordinates and time scales as

$$x \mapsto -x \frac{a_1}{g_1} \left(-\frac{g_1^2}{a_1 b_1} \right)^{4/5}, \quad y \mapsto y \left(-\frac{g_1^2}{a_1 b_1} \right)^{1/5}, \quad z \mapsto z \left(-\frac{g_1^2}{a_1 b_1} \right)^{2/5}, \quad t \mapsto -\frac{t}{g_1} \left(-\frac{g_1^2}{a_1 b_1} \right)^{2/5}, \quad (3.5)$$

and modifying the definitions of $h'_i s$ ($i = 1, \dots, 6$) appropriately, we obtain Eq.(3.1). \blacksquare

Let ρ_1 be a small positive number and let

$$\Sigma_{in}^+ = \{(X, Y, \rho_1^4) \mid (X, Y) \in \mathbf{R}^2\}, \quad \Sigma_{out}^+ = \{(X, \rho_1^2, Z) \mid (X, Z) \in \mathbf{R}^2\} \quad (3.6)$$

be Poincaré sections in the (X, Y, Z) space (see Fig.6). The purpose of this section is to construct a transition map from Σ_{in}^+ to Σ_{out}^+ . Recall that there exists a heteroclinic orbit α^+ emerging from L^+ , where L^+ corresponds to the origin in the (X, Y, Z) space.

Theorem 3.2. If $\rho_1 > 0$ is sufficiently small, there exists $\varepsilon_0 > 0$ such that the followings hold for $0 < \varepsilon < \varepsilon_0$:

(I) There exists an open set $U \subset \Sigma_{in}^+$ near the point $\Sigma_{in}^+ \cap S_a^+$ such that the transition map $\Pi_{loc}^+ : U \rightarrow \Sigma_{out}^+$ along the flow of Eq.(3.1) is well-defined and expressed as

$$\Pi_{loc}^+ \begin{pmatrix} X \\ Y \\ \rho_1^4 \end{pmatrix} = \begin{pmatrix} G_1(\rho_1) \\ \rho_1^2 \\ 0 \end{pmatrix} + \begin{pmatrix} G_2(\mathcal{X}, \mathcal{Y})\varepsilon^{4/5} + O(\varepsilon \log \varepsilon) \\ 0 \\ (\Omega + H(\mathcal{X}, \mathcal{Y}))\varepsilon^{4/5} + O(\varepsilon \log \varepsilon) \end{pmatrix}, \quad (3.7)$$

where $\Omega \sim -3.416$ is a negative constant, G_1, G_2, H are C^∞ functions, and \mathcal{X}, \mathcal{Y} are defined by

$$\begin{cases} \mathcal{X} = (D_1X + D_2Y)\varepsilon^{-3/5} \exp\left[-\frac{dc_1\rho_1}{\varepsilon}\right], \\ \mathcal{Y} = (D_3X + D_4Y)\varepsilon^{-2/5} \exp\left[-\frac{dc_1\rho_1}{\varepsilon}\right], \end{cases} \quad (3.8)$$

with some constants D_1, \dots, D_4 and $d > 0$.

(II) The point $(G_1(\rho_1), \rho_1^2, 0)$ is the intersection of α^+ and Σ_{out}^+ .

(III) The function H satisfies

$$H(0, 0) = 0, \quad \frac{\partial}{\partial \mathcal{X}} \Big|_{\mathcal{X}=0} H(\mathcal{X}, \mathcal{Y}) \neq 0. \quad (3.9)$$

This theorem means that an orbit of Eq.(1.5) or Eq.(3.1) running around S_a^+ goes to the right of L^+ and the distance of the orbit and the heteroclinic orbit α^+ is of $O(\varepsilon^{4/5})$. In particular, it converges to α^+ as $\varepsilon \rightarrow 0$. We use the blow-up method to prove this theorem. In Sec.3.2, we introduce the blow-up coordinates and outline the strategy of the proof of Thm.3.2. Analysis of our system in the blow-up coordinates is done after Sec.3.3 and the proof is completed in Sec.3.6. The constant Ω is a pole of the first Painlevé equation, as is shown in Sec.3.3. Eq.(3.9) is used in Sec.4 to prove Theorem 2.

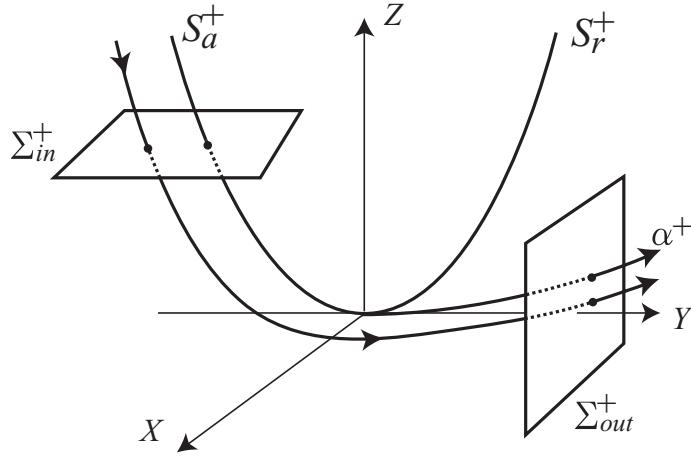


Fig. 6 Transition map Π_{loc}^+ and the heteroclinic orbit α^+ .

3.2 Blow-up coordinates

In this subsection, we introduce the blow-up coordinates to “desingularize” the fixed point L^+ having a nilpotent linear part. Regarding ε as a dependent variable on t , we rewrite Eq.(3.1) as

$$\begin{cases} \dot{X} = Z - Y^2 + c_1XY + c_2\varepsilon + Zh_1(X, Y, Z) + Y^2h_2(X, Y, Z) + \varepsilon h_3(X, Y, Z, \varepsilon), \\ \dot{Y} = -X + c_3\varepsilon + Zh_4(X, Y, Z) + \varepsilon h_5(X, Y, Z, \varepsilon), \\ \dot{Z} = -\varepsilon + \varepsilon h_6(X, Y, Z, \varepsilon), \\ \dot{\varepsilon} = 0. \end{cases} \quad (3.10)$$

For this system, we define the blow-up transformations K_1, K_2 and K_3 to be

$$(X, Y, Z, \varepsilon) = (r_1^3x_1, r_1^2y_1, r_1^4, r_1^5\varepsilon_1), \quad (3.11)$$

$$(X, Y, Z, \varepsilon) = (r_2^3x_2, r_2^2y_2, r_2^4z_2, r_2^5), \quad (3.12)$$

$$(X, Y, Z, \varepsilon) = (r_3^3x_3, r_3^2, r_3^4z_3, r_3^5\varepsilon_3), \quad (3.13)$$

respectively, where K_1, K_2 and K_3 are defined on half spaces $\{Z \geq 0\}$, $\{\varepsilon \geq 0\}$ and $\{Y \geq 0\}$, respectively. In what follows, we refer to the coordinates $(x_1, y_1, r_1, \varepsilon_1), (x_2, y_2, z_2, r_2), (x_3, r_3, z_3, \varepsilon_3)$ as K_1, K_2, K_3 coordinates, respectively. Transformations κ_{ij} from the K_i coordinates to the K_j

coordinates are given by

$$\begin{cases} K_{12} : (x_2, y_2, z_2, r_2) = (x_1 \varepsilon_1^{-3/5}, y_1 \varepsilon_1^{-2/5}, \varepsilon_1^{-4/5}, r_1 \varepsilon_1^{1/5}), \\ K_{21} : (x_1, y_1, r_1, \varepsilon_1) = (x_2 z_2^{-3/4}, y_2 z_2^{-1/2}, r_2 z_2^{1/4}, z_2^{-5/4}), \\ K_{32} : (x_2, y_2, z_2, r_2) = (x_3 \varepsilon_3^{-3/5}, \varepsilon_3^{-2/5}, z_3 \varepsilon_3^{-4/5}, r_3 \varepsilon_3^{1/5}), \\ K_{23} : (x_3, r_3, z_3, \varepsilon_3) = (x_2 y_2^{-3/2}, r_2 y_2^{1/2}, z_2 y_2^{-2}, y_2^{-5/2}), \end{cases} \quad (3.14)$$

respectively. Our next task is to write out Eq.(3.10) in the K_i coordinate. Eqs.(3.11) and (3.10) are put together to provide

$$\begin{cases} \dot{x}_1 = r_1(1 - y_1^2 + c_1 r_1 x_1 y_1 + c_2 r_1 \varepsilon_1 + \frac{3}{4} x_1 \varepsilon_1 + r_1^2 h_7(x_1, y_1, r_1, \varepsilon_1)), \\ \dot{y}_1 = r_1(-x_1 + \frac{1}{2} y_1 \varepsilon_1 + c_3 r_1^2 \varepsilon_1 + r_1^2 y_1 h_8(x_1, y_1, r_1, \varepsilon_1) + r_1^3 h_9(x_1, y_1, r_1, \varepsilon_1)), \\ \dot{r}_1 = -\frac{1}{4} r_1^2 \varepsilon_1 (1 - r_1^2 h_{10}(x_1, y_1, r_1, \varepsilon_1)), \\ \dot{\varepsilon}_1 = \frac{5}{4} r_1 \varepsilon_1^2 (1 - r_1^2 h_{10}(x_1, y_1, r_1, \varepsilon_1)), \end{cases} \quad (3.15)$$

where $h_7, h_8, h_9, h_{10} \sim O_p(1)$ are C^∞ functions. By changing the time scale appropriately, we can factor out r_1 in the right hand side of the above equations:

$$(K_1) \begin{cases} \dot{x}_1 = 1 - y_1^2 + c_1 r_1 x_1 y_1 + c_2 r_1 \varepsilon_1 + \frac{3}{4} x_1 \varepsilon_1 + r_1^2 h_7(x_1, y_1, r_1, \varepsilon_1), \\ \dot{y}_1 = -x_1 + \frac{1}{2} y_1 \varepsilon_1 + c_3 r_1^2 \varepsilon_1 + r_1^2 y_1 h_8(x_1, y_1, r_1, \varepsilon_1) + r_1^3 h_9(x_1, y_1, r_1, \varepsilon_1), \\ \dot{r}_1 = -\frac{1}{4} r_1 \varepsilon_1 (1 - r_1^2 h_{10}(x_1, y_1, r_1, \varepsilon_1)), \\ \dot{\varepsilon}_1 = \frac{5}{4} \varepsilon_1^2 (1 - r_1^2 h_{10}(x_1, y_1, r_1, \varepsilon_1)). \end{cases} \quad (3.16)$$

Since the time scale transformation does not change the phase portrait of Eq.(3.15), we can use Eq.(3.16) to calculate the transition map.

In a similar manner (*i.e.* changing the coordinates and dividing by the common factors), we obtain the systems of equations written in the K_2, K_3 coordinates as

$$(K_2) \begin{cases} \dot{x}_2 = z_2 - y_2^2 + c_1 r_2 x_2 y_2 + c_2 r_2 + r_2^2 h_{12}(x_2, y_2, z_2, r_2), \\ \dot{y}_2 = -x_2 + c_3 r_2^2 + r_2^3 h_{13}(x_2, y_2, z_2, r_2), \\ \dot{z}_2 = -1 + r_2^2 h_{14}(x_2, y_2, z_2, r_2), \\ \dot{r}_2 = 0, \end{cases} \quad (3.17)$$

and

$$(K_3) \begin{cases} \dot{x}_3 = -1 + z_3 + c_1 r_3 x_3 + c_2 r_3 \varepsilon_3 + \frac{3}{2} x_3 h_{18}(x_3, r_3, z_3, \varepsilon_3) + r_3^2 h_{15}(x_3, r_3, z_3, \varepsilon_3), \\ \dot{r}_3 = -\frac{1}{2} r_3 h_{18}(x_3, r_3, z_3, \varepsilon_3), \\ \dot{z}_3 = -\varepsilon_3 + 2z_3 h_{18}(x_3, r_3, z_3, \varepsilon_3) + r_3^2 \varepsilon_3 h_{16}(x_3, r_3, z_3, \varepsilon_3), \\ \dot{\varepsilon}_3 = \frac{5}{2} \varepsilon_3 h_{18}(x_3, r_3, z_3, \varepsilon_3), \end{cases} \quad (3.18)$$

respectively, where $h_{18}(x_3, r_3, z_3, \varepsilon_3) := x_3 + r_3^2 h_{17}(x_3, r_3, z_3, \varepsilon_3)$ and $h_i \sim O_p(1)$ ($i = 12, \dots, 17$) are C^∞ functions.

Our strategy for understanding the flow of Eq.(3.1) near the fold points L^+ is as follows: In Sec.3.3, we analyze Eq.(3.17) in the K_2 coordinates. We will find it to be a perturbed first Painlevé equation. Since asymptotic behavior of the first Painlevé equation is well studied, we can construct a transition map along the flow of it approximately. In Sec.3.4, we analyze Eq.(3.16) in the K_1 coordinates. We will see that S_a^+ has a 2-dimensional attracting center manifold W^c (see Fig.7). Since it is attracting, orbits passing nearby S_a^+ approaches W^c . Thus if we construct the invariant manifold W^c globally, we can well understand asymptotic behavior of orbits passing through nearby S_a^+ . Although usual center manifold theory provides the center manifold W^c only locally, we will show that there exists an orbit γ of the first Painlevé equation in the K_2 coordinates such that if it is transformed into the K_1 coordinates, it is attached on the edge of W^c (see Fig.7). This means that the orbit γ of the first Painlevé equation guides the manifold W^c and provides a global structure of it. In Sec.3.5, we analyze Eq.(3.18) in the K_3 coordinates. We will see that there exists a fixed point whose unstable manifold is 1-dimensional. Since the orbit γ of the first Painlevé equation written in the K_3 coordinates approaches the fixed point, the manifold W^c put on the γ is also attached on the unstable manifold (see Fig.7). The unstable manifold corresponds to the heteroclinic orbit α^+ in the (X, Y, Z) coordinates if it is blown down. This means that orbits of Eq.(3.1) coming from a region above L^+ go to the right of L^+ (see Fig.6) and pass near the heteroclinic orbit α^+ . Thus the transition map Π_{loc}^+ is well defined.

Combining transition maps constructed on each K_i coordinates and blowing it down to the (X, Y, Z) coordinates, we can prove Thm.3.2.

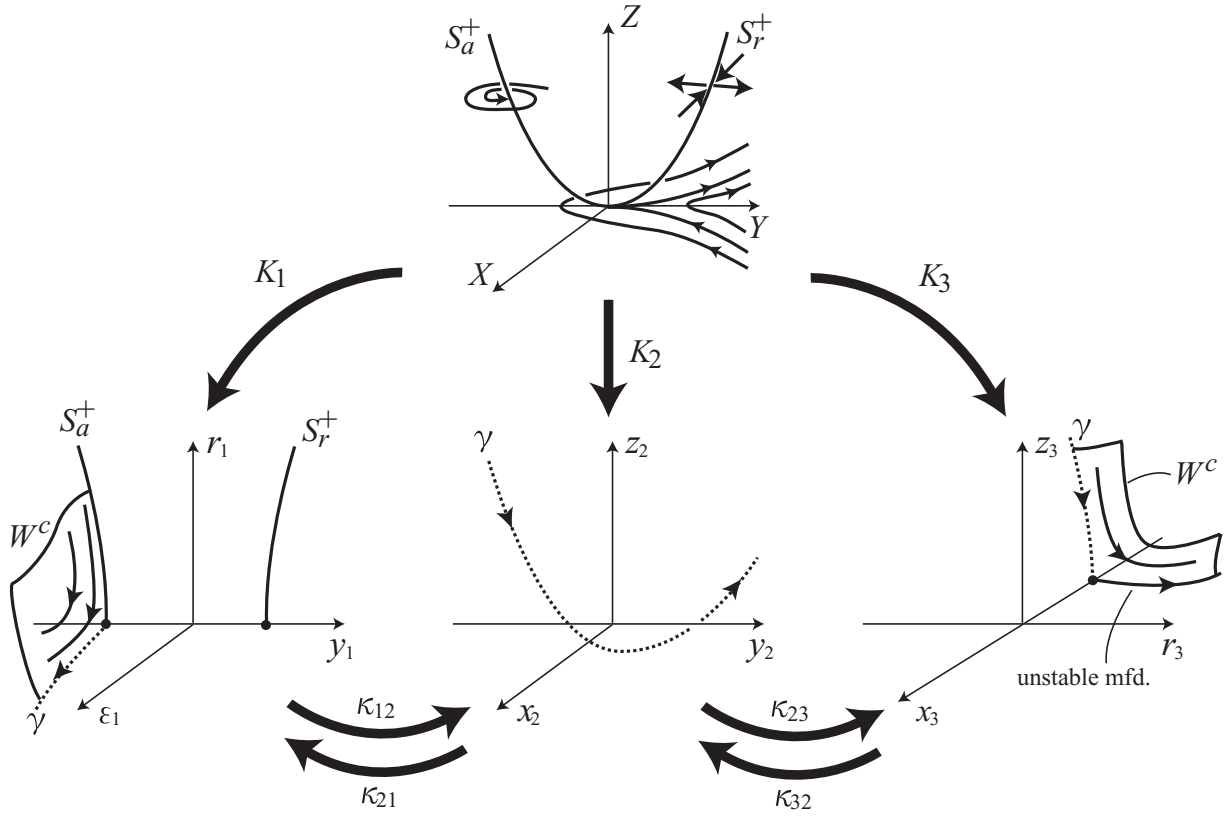


Fig. 7 The flow in the (X, Y, Z) coordinates and the blow-up coordinates. The dotted line denotes the orbit γ of the first Painlevé equation.

3.3 Analysis in the K_2 coordinates

We consider Eq.(3.17). Since $r_2 = \varepsilon^{1/5}$ is a small constant, we are allowed to take the system

$$\begin{cases} \dot{x}_2 = z_2 - y_2^2, \\ \dot{y}_2 = -x_2, \\ \dot{z}_2 = -1, \end{cases} \quad (3.19)$$

as the unperturbed system of Eq.(3.17). This is equivalent to the first Painlevé equation :

$$\begin{cases} \frac{dx_2}{dz_2} = -z_2 + y_2^2, \\ \frac{dy_2}{dz_2} = x_2, \end{cases} \quad \text{or} \quad \frac{d^2 y_2}{dz_2^2} = -z_2 + y_2^2. \quad (3.20)$$

It is known that there exists a two parameter family of solutions of the first Painlevé equation whose asymptotic expansions are given by

$$\begin{pmatrix} x_2(z_2) \\ y_2(z_2) \end{pmatrix} = \begin{pmatrix} -\frac{1}{2}z_2^{-1/2} - \left(\frac{C_1}{8}z_2^{-9/8} - \sqrt{2}C_2z_2^{1/8}\right)\cos\phi - \left(\frac{C_2}{8}z_2^{-9/8} + \sqrt{2}C_1z_2^{1/8}\right)\sin\phi + O(z_2^{-3}) \\ -z_2^{1/2} + C_1z_2^{-1/8}\cos\phi + C_2z_2^{-1/8}\sin\phi + O(z_2^{-2}) \end{pmatrix}, \quad (3.21)$$

as $z_2 \rightarrow \infty$ and

$$\begin{pmatrix} x_2(z_2) \\ y_2(z_2) \end{pmatrix} = \begin{pmatrix} \frac{-12}{(z_2 - z_0)^3} + \frac{z_0}{5}(z_2 - z_0) + \frac{1}{2}(z_2 - z_0)^2 + 4C_3(z_2 - z_0)^3 + O((z_2 - z_0)^4) \\ \frac{6}{(z_2 - z_0)^2} + \frac{z_0}{10}(z_2 - z_0)^2 + \frac{1}{6}(z_2 - z_0)^3 + C_3(z_2 - z_0)^4 + O((z_2 - z_0)^5) \end{pmatrix}, \quad (3.22)$$

as $z_2 \rightarrow z_0 + 0$, where $\phi \sim \frac{4\sqrt{2}}{5}z_2^{5/4}$ ($z_2 \rightarrow \infty$), and where C_1, C_2, C_3 and z_0 are constants which depend on an initial value. The value z_0 is a movable pole of the first Painlevé equation (see Ince [9], Noonburg [14]). In particular, there exists a solution γ whose asymptotic expansions as $z_2 \rightarrow \infty$ and as $z_2 \rightarrow \Omega + 0$ are of the form

$$\gamma : \begin{pmatrix} x_2 \\ y_2 \end{pmatrix} = \begin{pmatrix} x_2(z_2) \\ y_2(z_2) \end{pmatrix} = \begin{pmatrix} -\frac{1}{2}z_2^{-1/2} + O(z_2^{-3}) \\ -z_2^{1/2} + O(z_2^{-2}) \end{pmatrix}, \quad (3.23)$$

and

$$\gamma : \begin{pmatrix} x_2 \\ y_2 \end{pmatrix} = \begin{pmatrix} x_2(z_2) \\ y_2(z_2) \end{pmatrix} = \begin{pmatrix} \frac{-12}{(z_2 - \Omega)^3} + \frac{\Omega}{5}(z_2 - \Omega) + O((z_2 - \Omega)^2) \\ \frac{6}{(z_2 - \Omega)^2} + \frac{\Omega}{10}(z_2 - \Omega)^2 + O((z_2 - \Omega)^3) \end{pmatrix}, \quad (3.24)$$

respectively, where $\Omega \sim -3.416$ is the pole of Eq.(3.20).

Let ρ_2 and ρ_3 be small positive numbers and define Poincaré sections to be

$$\Sigma_2^{in} = \{z_2 = \rho_2^{-4/5}\}, \quad \Sigma_2^{out} = \{y_2 = \rho_3^{-2/5}\}, \quad (3.25)$$

(see Fig.8). By Eqs.(3.23, 24), the intersections $P_2 = \gamma \cap \Sigma_2^{out}$, $Q_2 = \gamma \cap \Sigma_2^{in}$ of γ and the sections are given by

$$P_2 = (p_x, p_y, p_z) = \left((2/3)^{1/2}\rho_3^{-3/5} + O(\rho_3^{1/5}), \rho_3^{-2/5}, \Omega + \sqrt{6}\rho_3^{1/5} + O(\rho_3) \right), \quad (3.26)$$

$$Q_2 = (q_x, q_y, q_z) = \left(-\rho_2^{2/5}/2 + O(\rho_2^{12/5}), -\rho_2^{-2/5} + O(\rho_2^{8/5}), \rho_2^{-4/5} \right), \quad (3.27)$$

respectively.

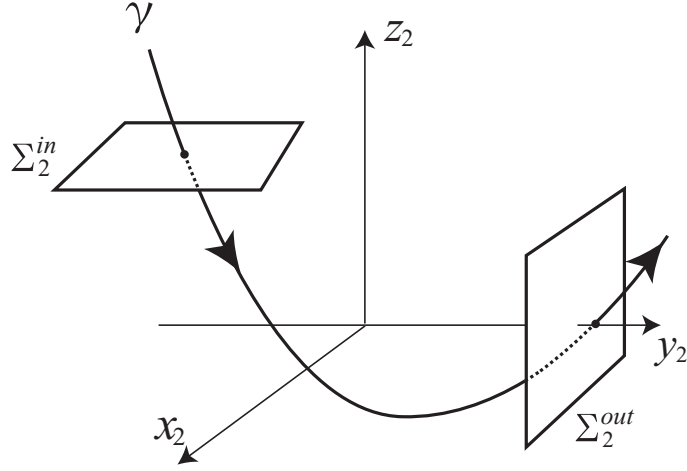


Fig. 8 The solution γ of the first Painlevé equation and the Poincaré sections.

Proposition 3.3. There exists an open set $U_2 \subset \Sigma_2^{in}$ such that the transition map $\Pi_2^{loc} : U_2 \rightarrow \Sigma_2^{out}$ along the flow of Eq.(3.17) is well-defined and expressed as

$$\Pi_2^{loc} \begin{pmatrix} x_2 \\ y_2 \\ \rho_2^{-4/5} \\ r_2 \end{pmatrix} = \begin{pmatrix} p_x \\ p_y \\ p_z \\ 0 \end{pmatrix} + \begin{pmatrix} H_1(x_2 - q_x, y_2 - q_y, r_2, \rho_3) \\ 0 \\ H_2(x_2 - q_x, y_2 - q_y, r_2, \rho_3) \\ r_2 \end{pmatrix}, \quad (3.28)$$

where $H_1(x, y, r, \rho_3)$ and $H_2(x, y, r, \rho_3)$ are C^∞ functions of x, y, r and they satisfy the equalities $H_1(0, 0, 0, \rho_3) = H_2(0, 0, 0, \rho_3) = 0$ for any small ρ_3 .

Proof. This is an immediate consequence of the continuity of solutions with respect to initial values and a parameter r_2 . ■

Since H_1 and H_2 are C^∞ with respect to r , we put them in the form

$$H_i(x, y, r, \rho_3) = \tilde{H}_i(x, y, \rho_3) + O(r), \quad i = 1, 2. \quad (3.29)$$

Then, the value $\lim_{\rho_3 \rightarrow 0} (p_z + \tilde{H}_2(x - q_x, y - q_y, \rho_3))$ gives a pole to which an orbit of Eq.(3.20) through an initial point $(x, y, \rho_2^{-4/5})$ converges as z_2 decreases.

The next lemma is used to prove Thm.3.2 (III).

Lemma 3.4. The function \tilde{H}_2 satisfies the following:

- (i) $\lim_{\rho_3 \rightarrow 0} \tilde{H}_2(x_2 - q_x, y_2 - q_y, \rho_3) \neq 0$ for generic points with $(x_2, y_2) \neq (q_x, q_y)$,

- (ii) $\frac{\partial}{\partial x}\Big|_{x=0} \tilde{H}_2(x, y, \rho_3) \neq 0$ for small $\rho_3 > 0$,
- (iii) \tilde{H}_2 is C^1 with respect to small $\eta := \rho_3^{1/5} > 0$,
- (iv) $\lim_{\rho_3 \rightarrow 0} \frac{\partial}{\partial x}\Big|_{x=0} \tilde{H}_2(x, y, \rho_3) \neq 0$.

Proof. (i) This follows from the well known fact that the Painlevé equation has a movable pole (*i.e.* the value z_0 in Eq.(3.22) depends on an initial value (x_2, y_2)).

(ii) Eq.(3.20) can be written in the Hamiltonian form $dx_2/dz_2 = -\partial\mathcal{K}/\partial y_2$, $dy_2/dz_2 = \partial\mathcal{K}/\partial x_2$ with the Hamiltonian function $\mathcal{K} = x_2^2/2 + y_2 z_2 - y_2^3/3$, so that any solutions $(x_2(z_2), y_2(z_2))$ of Eq.(3.20) satisfies the equality

$$\frac{1}{2}(x_2(b)^2 - x_2(a)^2) + (by_2(b) - ay_2(a)) - \frac{1}{3}(y_2(b)^3 - y_2(a)^3) = \int_a^b y_2(z)dz, \quad (3.30)$$

for any $b > a$. Let $(x_2(z_2), y_2(z_2))$ be a solution of Eq.(3.20) whose initial value is $(x, y, \rho_2^{-4/5}, 0) \in U_2$, and put

$$\Pi_2^{loc}(x, y, \rho_2^{-4/5}, 0) = (\Pi_x(x, y), \rho_3^{-2/5}, \Pi_z(x, y), 0).$$

Then, Eq.(3.30) provides

$$\frac{1}{2}(x^2 - \Pi_x(x, y)^2) + (\rho_2^{-4/5}y - \rho_3^{-2/5}\Pi_z(x, y)) - \frac{1}{3}(y^3 - \rho_3^{-6/5}) = \int_{\Pi_z(x, y)}^{\rho_2^{-4/5}} y_2(z)dz. \quad (3.31)$$

Differentiating the above with respect to x yields

$$x - \Pi_x(x, y) \frac{\partial}{\partial x} \Pi_x(x, y) - \rho_3^{-2/5} \frac{\partial}{\partial x} \Pi_z(x, y) = \int_{\Pi_z(x, y)}^{\rho_2^{-4/5}} \frac{\partial}{\partial x} y_2(z) dz - \rho_3^{-2/5} \frac{\partial}{\partial x} \Pi_z(x, y), \quad (3.32)$$

where $\partial\Pi_x/\partial x$ is calculated as

$$\begin{aligned} \frac{\partial}{\partial x} \Pi_x(x, y) &= \frac{\partial}{\partial x} x_2(\Pi_z(x, y)) \\ &= \frac{\partial}{\partial z}\Big|_{z=\Pi_z(x, y)} x_2(z) \cdot \frac{\partial}{\partial x} \Pi_z(x, y) \\ &= (y_2(\Pi_z(x, y))^2 - \Pi_z(x, y)) \cdot \frac{\partial}{\partial x} \Pi_z(x, y). \end{aligned} \quad (3.33)$$

For fixed $\rho_3 > 0$, if we assume that

$$\frac{\partial}{\partial x}\Big|_{x=q_x} \Pi_z(x, y) = 0, \quad (3.34)$$

then Eq.(3.32) with Eq.(3.33) provides

$$q_x = \int_{\Pi_z(q_x, y)}^{\rho_2^{-4/5}} \frac{\partial}{\partial x} \Big|_{x=q_x} y_2(z) dz. \quad (3.35)$$

However, this is a contradiction; though the right hand side of the above clearly depends on ρ_3 through $\Pi_z(q_x, y)$, left hand side does not. Thus the left hand side of Eq.(3.34) is nonzero. This proves (ii) of Lemma 3.4.

(iii) Differentiating Eq.(3.31) with respect to $\eta = \rho_3^{1/5}$ provides

$$-\Pi_x(x, y) \frac{\partial \Pi_x}{\partial \eta}(x, y) + 2\eta^{-3} \Pi_z(x, y) - 2\eta^{-7} = 0. \quad (3.36)$$

Since $\partial \Pi_x / \partial \eta$ is evaluated in a similar manner to that for Eq.(3.33) and since $\Pi_z(x, y) = \Omega + O(\eta) + \tilde{H}_2(x - q_x, y - q_y, \rho_3)$ and $\Pi_x(x, y) = \sqrt{2/3} \eta^{-3} + O(\eta) + \tilde{H}_1(x - q_x, y - q_y, \rho_3)$, Eq.(3.36) is brought into

$$\begin{aligned} & -\eta^7 \left(\sqrt{\frac{2}{3}} \eta^{-3} + O(\eta) + \tilde{H}_1(x - q_x, y - q_y, \rho_3) \right) \left(\eta^{-4} - \Omega + O(\eta) - \tilde{H}_2(x - q_x, y - q_y, \rho_3) \right) \frac{\partial \Pi_z}{\partial \eta}(x, y) \\ & + 2\eta^4 \left(\Omega + O(\eta) + \tilde{H}_2(x - q_x, y - q_y, \rho_3) \right) = 2. \end{aligned} \quad (3.37)$$

It is easy to verify that $\tilde{H}_1(x, y, \rho_3)$ is bounded as $\rho_3 \rightarrow 0$ by using the asymptotic expansion (3.22) of solutions of Eq.(3.20) near a pole. Thus Eq.(3.37) implies that $\partial \Pi_z / \partial \eta$ exists for small η and in particular

$$\frac{\partial \Pi_z}{\partial \eta} \Big|_{\eta=0}(x, y) = -\sqrt{6}. \quad (3.38)$$

(iv) By (iii) of Lemma 3.4, \tilde{H}_2 is written as

$$\tilde{H}_2(x, y, \rho_3) = \hat{H}_2(x, y) + O(\rho_3^{1/5}), \quad (3.39)$$

with a C^∞ function \hat{H}_2 . Now (iv) of Lemma 3.4 follows from (ii) of that. \blacksquare

3.4 Analysis in the K_1 coordinates

We turn to Eq.(3.16). It is easy to verify that Eq.(3.16) has fixed points $(x_1, y_1, r_1, \varepsilon_1) = (0, \pm 1, 0, 0)$. By virtue of the implicit function theorem, we can show that there exist two sets of fixed points which form two curves emerging from $(0, \pm 1, 0, 0)$, and they correspond to S_a^+

and S_r^+ , respectively (see Fig.7). On the fixed points, the Jacobian matrix of the right hand side of Eq.(3.16) has eigenvalues given by

$$0, 0, \frac{1}{2} \left(c_1 r_1 y_1 + O(r_1^2) \pm \sqrt{8y_1 - 4c_1 r_1 x_1 + O(r_1^2)} \right). \quad (3.40)$$

In particular, the eigenvalues become $0, 0, \pm \sqrt{2}i$ at the fixed point $Q_1 = (0, -1, 0, 0)$, but at fixed points in $S_a^+ \setminus Q_1$, they have two eigenvalues whose real parts are negative if r_1 is small (recall that $c_1 > 0$). Eigenvectors associated with the two zero eigenvalues at points on $S_a^+ \setminus Q_1$ converge to those at Q_1 , which are given by $(0, 0, 1, 0)$ and $(-1, 0, 0, 2)$, as $r_1 \rightarrow 0$.

Lemma 3.5. There exists an attracting 2-dimensional center manifold W^c which includes S_a^+ and the orbit γ of the first Painlevé equation written in the K_1 coordinates (see Fig.9).

Proof. Let $B(a)$ be the open ball of radius a centered at Q_1 . Since at points in $S^+ \setminus B(a)$ the Jacobian matrix has two zero eigenvalues and the other two eigenvalues with negative real parts, there exists an attracting 2-dimensional center manifold $W^c(a)$ emerging from $S^+ \setminus B(a)$ for any small $a > 0$. Let γ be the solution of the first Painlevé equation described in the previous subsection. Its asymptotic expansion (3.23) is written in the K_1 coordinates as

$$\gamma : \begin{pmatrix} x_1 \\ y_1 \\ r_1 \\ \varepsilon_1 \end{pmatrix} = \begin{pmatrix} -\frac{1}{2}z_2^{-5/4} + O(z_2^{-15/4}) \\ -1 + O(z_2^{-5/2}) \\ 0 \\ z_2^{-5/4} \end{pmatrix} \quad (\text{as } z_2 \rightarrow \infty), \quad (3.41)$$

by the coordinate change κ_{21} (3.14). The curve (3.41) approaches the point Q_1 as $z_2 \rightarrow \infty$ and its tangent vector converges to the eigenvector $(-1, 0, 0, 2)$ at Q_1 as $z_2 \rightarrow \infty$. Thus $W^c := \lim_{a \rightarrow 0} W^c(a) \cup \gamma$ forms an invariant manifold. \blacksquare

This lemma means that the orbit γ guides global behavior of the center manifold W^c .

Let $\rho_1, \rho_2 > 0$ be the small constants referred to in Thm.3.2 and Lem.3.3, respectively. Take two Poincaré sections Σ_1^{in} and Σ_1^{out} defined to be

$$\begin{aligned} \Sigma_1^{in} &= \{(x_1, y_1, r_1, \varepsilon_1) \mid r_1 = \rho_1, |x_1| \leq \rho_1, |y_1 + 1| \leq \rho_1, 0 < \varepsilon_1 \leq \rho_2\}, \\ \Sigma_1^{out} &= \{(x_1, y_1, r_1, \varepsilon_1) \mid 0 \leq r_1 \leq \rho_1, |x_1| \leq \rho_1, |y_1 + 1| \leq \rho_1, \varepsilon_1 = \rho_2\}, \end{aligned} \quad (3.42)$$

respectively. Note that Σ_1^{in} is included in the section Σ_{in}^+ (see Eq.(3.6)) if written in the (X, Y, Z) coordinates and Σ_1^{out} in the section Σ_2^{in} (see Eq.(3.25)) if written in the K_2 coordinates.

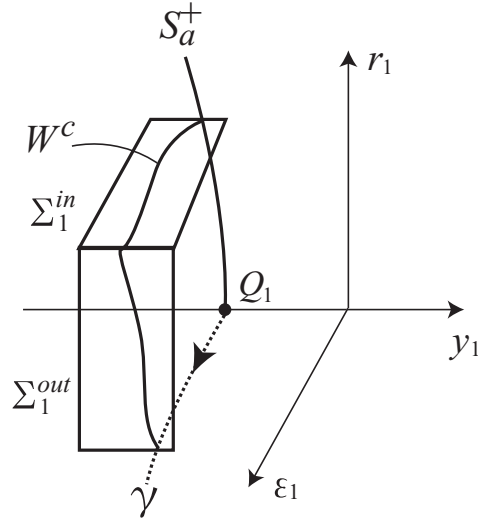


Fig. 9 Poincaré sections to define the transition map Π_1^{loc} .

Proposition 3.6. (I) If ρ_1 and ρ_2 are small, the transition map $\Pi_1^{loc} : \Sigma_1^{in} \rightarrow \Sigma_1^{out}$ along the flow of Eq.(3.16) is well-defined and expressed as

$$\Pi_1^{loc} \begin{pmatrix} x_1 \\ y_1 \\ \rho_1 \\ \varepsilon_1 \end{pmatrix} = \begin{pmatrix} \varphi_1(\rho_1 \varepsilon_1^{1/5} \rho_2^{-1/5}, \rho_2) \\ \varphi_2(\rho_1 \varepsilon_1^{1/5} \rho_2^{-1/5}, \rho_2) \\ \rho_1 \varepsilon_1^{1/5} \rho_2^{-1/5} \\ \rho_2 \end{pmatrix} + \begin{pmatrix} (1 + \beta_1(x_1, y_1, \rho_1, \varepsilon_1, \rho_2)) \tilde{X}_1 \\ (1 + \beta_2(x_1, y_1, \rho_1, \varepsilon_1, \rho_2)) \tilde{Y}_1 \\ 0 \\ 0 \end{pmatrix}, \quad (3.43)$$

where φ_1 and φ_2 are C^∞ functions such that the graph of $x_1 = \varphi_1(r_1, \varepsilon_1)$ and $y_1 = \varphi_2(r_1, \varepsilon_1)$ gives the center manifold W^c , \tilde{X}_1 and \tilde{Y}_1 are defined by

$$\begin{cases} \tilde{X}_1 = \tilde{X}_1(x_1, y_1, \rho_1, \varepsilon_1, \rho_2) = (D_1 x_1 + D_2 y_1) \left(\frac{\rho_2}{\varepsilon_1} \right)^{3/5} \exp\left[-\frac{dc_1 \rho_1}{\varepsilon_1}\right] (1 + O((\varepsilon_1/\rho_2)^{1/5})), \\ \tilde{Y}_1 = \tilde{Y}_1(x_1, y_1, \rho_1, \varepsilon_1, \rho_2) = (D_3 x_1 + D_4 y_1) \left(\frac{\rho_2}{\varepsilon_1} \right)^{2/5} \exp\left[-\frac{dc_1 \rho_1}{\varepsilon_1}\right] (1 + O((\varepsilon_1/\rho_2)^{1/5})), \end{cases} \quad (3.44)$$

with some constants D_i ($i = 1, \dots, 4$) and $d > 0$, and where β_1, β_2 are C^∞ functions with respect to x_1, y_1 and ρ_1 which are sufficiently smaller than 1 if ρ_1, ρ_2 and ε_1 are sufficiently small.

(II) The first term in the right hand side of Eq.(3.43) is on the intersection of Σ_1^{out} and the center manifold W^c . In particular, as $\varepsilon_1 \rightarrow 0$, $\Pi_1^{loc}(x_1, y_1, \rho_1, \varepsilon_1)$ converges to the intersection point of Σ_1^{out} and γ .

Proof. At first, we divide the right hand side of Eq.(3.16) by $1 - r_1^2 h_{10}$ and change the time scale accordingly. Note that this does not change the phase portrait. Then we obtain

$$\begin{cases} \dot{x}_1 = 1 - y_1^2 + c_1 r_1 x_1 y_1 + c_2 r_1 \varepsilon_1 + \frac{3}{4} x_1 \varepsilon_1 + r_1^2 h_{21}(x_1, y_1, r_1, \varepsilon_1), \\ \dot{y}_1 = -x_1 + \frac{1}{2} y_1 \varepsilon_1 + r_1^2 h_{22}(x_1, y_1, r_1, \varepsilon_1), \\ \dot{r}_1 = -\frac{1}{4} r_1 \varepsilon_1, \\ \dot{\varepsilon}_1 = \frac{5}{4} \varepsilon_1^2, \end{cases} \quad (3.45)$$

where $h_{21}, h_{22} \sim O_p(1)$ are C^∞ functions. Equations for r_1 and ε_1 are solved as

$$r_1(t) = r_1(0) \left(\frac{4 - 5\varepsilon_1(0)t}{4} \right)^{1/5}, \quad \varepsilon_1(t) = \frac{4\varepsilon_1(0)}{4 - 5\varepsilon_1(0)t}, \quad (3.46)$$

respectively. Let T be a transition time from Σ_1^{in} to Σ_1^{out} . Since $\varepsilon_1(T) = \rho_2$, T is given by

$$T = \frac{4}{5\varepsilon_1(0)} \left(1 - \frac{\varepsilon_1(0)}{\rho_2} \right). \quad (3.47)$$

The center manifold W^c is given as a graph of C^∞ functions $x_1 = \varphi_1(r_1, \varepsilon_1)$, $y_1 = \varphi_2(r_1, \varepsilon_1)$. By using the standard center manifold theory, we can calculate φ_1 and φ_2 as

$$\varphi_1(r_1, \varepsilon_1) = -\frac{1}{2} \varepsilon_1 + O(r_1^2, r_1 \varepsilon_1, \varepsilon_1^2), \quad \varphi_2(r_1, \varepsilon_1) = -1 + O(r_1^2, r_1 \varepsilon_1, \varepsilon_1^2). \quad (3.48)$$

To see the behavior of solutions $x_1(t)$ and $y_1(t)$ near the center manifold W^c , we put $x_1(t)$ and $y_1(t)$ in the form

$$x_1(t) = X_1(t) + \varphi_1(r_1(t), \varepsilon_1(t)), \quad y_1(t) = Y_1(t) + \varphi_2(r_1(t), \varepsilon_1(t)). \quad (3.49)$$

Then Eq.(3.45) yields the equations for $X_1(t)$ and $Y_1(t)$

$$\begin{cases} \dot{X}_1 = 2Y_1 - c_1 r_1(t) X_1 + \frac{3}{4} \varepsilon_1(t) X_1 - Y_1^2 + h_{23}(X_1, Y_1, r_1, \varepsilon_1), \\ \dot{Y}_1 = -X_1 + \frac{1}{2} \varepsilon_1(t) Y_1 + h_{24}(X_1, Y_1, r_1, \varepsilon_1), \end{cases} \quad (3.50)$$

where $h_{23}, h_{24} \sim O_p(3)$ are C^∞ functions. We note here that solutions $X_1(t)$ and $Y_1(t)$ are exponentially small because the center manifold W^c is attracting. In particular, since the negative real parts of eigenvalues of the fixed points on $S_a^+ \setminus Q_1$ are of order $O(-c_1 r_1)$ (see Eq.(3.40)), solutions behave like $X_1(t), Y_1(t) \sim t^m e^{-dc_1 r_1(0)t}$ when t is large, where m and

$d > 0$ are some real numbers. We proceed to estimate the m by using the theory of ODEs in the complex domain. In view of Eq.(3.50), we consider the truncated system of the form

$$\begin{cases} \dot{\tilde{X}}_1 = 2\tilde{Y}_1 - c_1 r_1(t)\tilde{X}_1 + \frac{3}{4}\varepsilon_1(t)\tilde{X}_1, \\ \dot{\tilde{Y}}_1 = -\tilde{X}_1 + \frac{1}{2}\varepsilon_1(t)\tilde{Y}_1. \end{cases} \quad (3.51)$$

On introducing the new time variable τ by

$$\tau = \left(\frac{4 - 5\varepsilon_1(0)t}{4} \right)^{1/5}, \quad (3.52)$$

the above system is rewritten as

$$\frac{d}{d\tau} \begin{pmatrix} \tilde{X}_1 \\ \tilde{Y}_1 \end{pmatrix} = \frac{1}{\tau} \begin{pmatrix} -3 & 0 \\ 0 & -2 \end{pmatrix} \begin{pmatrix} \tilde{X}_1 \\ \tilde{Y}_1 \end{pmatrix} + \tau^4 \frac{4}{\varepsilon_1(0)} \begin{pmatrix} 0 & -2 \\ 1 & 0 \end{pmatrix} \begin{pmatrix} \tilde{X}_1 \\ \tilde{Y}_1 \end{pmatrix} + \tau^5 \frac{4c_1 r_1(0)}{\varepsilon_1(0)} \begin{pmatrix} 1 & 0 \\ 0 & 0 \end{pmatrix} \begin{pmatrix} \tilde{X}_1 \\ \tilde{Y}_1 \end{pmatrix}. \quad (3.53)$$

It is easy to verify that this system has solutions of the form

$$\begin{pmatrix} \tilde{X}_1(t) \\ \tilde{Y}_1(t) \end{pmatrix} = MR(\tau)R(1)^{-1} \begin{pmatrix} \tilde{X}_1(0) \\ \tilde{Y}_1(0) \end{pmatrix}, \quad M := \begin{pmatrix} \tau^{-3} & 0 \\ 0 & \tau^{-2} \end{pmatrix}, \quad (3.54)$$

where M is the monodromy matrix and $R(\tau) = \sum_{k=0}^{\infty} R_k \tau^k$ is a matrix-valued entire function satisfying $R(0) = id$. When $t = T$, one has $\tau = (\varepsilon_1/\rho_2)^{1/5}$ and then the above solution is estimated as

$$\begin{aligned} \begin{pmatrix} \tilde{X}_1(T) \\ \tilde{Y}_1(T) \end{pmatrix} &= \begin{pmatrix} (\rho_2/\varepsilon_1)^{3/5} & 0 \\ 0 & (\rho_2/\varepsilon_1)^{2/5} \end{pmatrix} R((\varepsilon_1/\rho_2)^{1/5}) R(1)^{-1} \begin{pmatrix} \tilde{X}_1(0) \\ \tilde{Y}_1(0) \end{pmatrix} \\ &= \begin{pmatrix} (\rho_2/\varepsilon_1)^{3/5} & 0 \\ 0 & (\rho_2/\varepsilon_1)^{2/5} \end{pmatrix} R(1)^{-1} (id + O((\varepsilon_1/\rho_2)^{1/5})) \begin{pmatrix} \tilde{X}_1(0) \\ \tilde{Y}_1(0) \end{pmatrix}. \end{aligned} \quad (3.55)$$

Since the center manifold theory manifests that $\tilde{X}_1(t)$ and $\tilde{Y}_1(t)$ decay exponentially like $\sim e^{-dc_1 r_1(0)t}$, there exist constants D_i ($i = 1, \dots, 4$) and $d > 0$ such that

$$\begin{cases} \tilde{X}_1(T) = (D_1 \tilde{X}_1(0) + D_2 \tilde{Y}(0)) \left(\frac{\rho_2}{\varepsilon_1} \right)^{3/5} \exp[-dc_1 r_1(0)T] (1 + O(\varepsilon_1/\rho_2)^{1/5}), \\ \tilde{Y}_1(T) = (D_3 \tilde{X}_1(0) + D_4 \tilde{Y}(0)) \left(\frac{\rho_2}{\varepsilon_1} \right)^{2/5} \exp[-dc_1 r_1(0)T] (1 + O(\varepsilon_1/\rho_2)^{1/5}). \end{cases} \quad (3.56)$$

Now the variation-of-constants formula applied to Eq.(3.50) results in Eq.(3.43). Proposition 3.6 (II) is clear from the definition of φ_1 and φ_2 . ■

3.5 Analysis in the K_3 coordinates

We come to the system (3.18). This system has the fixed point $(x_3, r_3, z_3, \varepsilon_3) = (-\sqrt{2/3}, 0, 0, 0)$ (see Fig.7). To analyze the system, we divide the right hand side of Eq.(3.18) by $-h_{18}(x_3, r_3, z_3, \varepsilon_3)$ and change the time scale accordingly. Note that this does not change the phase portrait. At first, note that the equality

$$\frac{1}{h_{18}(x_3, r_3, z_3, \varepsilon_3)} = -\sqrt{\frac{3}{2}} \left(1 + \sqrt{\frac{3}{2}} \left(x_3 + \sqrt{\frac{2}{3}} \right) + h_{29}(x_3 + \sqrt{2/3}, r_3, z_3, \varepsilon_3) \right) \quad (3.57)$$

holds, where $h_{29} \sim O_p(2)$ is a C^∞ function. Using Eq.(3.57) and introducing the new coordinate by $x_3 + \sqrt{2/3} = \tilde{x}_3$, we eventually obtain

$$\begin{cases} \dot{\tilde{x}}_3 = -3\tilde{x}_3 + \sqrt{\frac{3}{2}}z_3 - c_1r_3 + h_{30}(\tilde{x}_3, r_3, z_3, \varepsilon_3), \\ \dot{r}_3 = \frac{1}{2}r_3, \\ \dot{z}_3 = -2z_3 - \sqrt{\frac{3}{2}}\varepsilon_3 + \varepsilon_3h_{31}(\tilde{x}_3, z_3, \varepsilon_3) + \varepsilon_3r_3h_{32}(\tilde{x}_3, r_3, z_3, \varepsilon_3), \\ \dot{\varepsilon}_3 = -\frac{5}{2}\varepsilon_3, \end{cases} \quad (3.58)$$

where $h_{30} \sim O_p(2)$ and $h_{31}, h_{32} \sim O_p(1)$ are C^∞ functions. This system has a fixed point at the origin, and eigenvalues of the Jacobian matrix at the origin of the right hand side of Eq.(3.58) are given by $-3, 1/2, -2, -5/2$. In particular, the eigenvector associated with the positive eigenvalue $1/2$ is given by $(-2c_1/7, 1, 0, 0)$ and the origin has a 1-dimensional unstable manifold which is tangent to the eigenvector. The asymptotic expansion (3.24) of the solution γ of the first Painlevé equation is rewritten in the present coordinates as

$$(\tilde{x}_3, r_3, z_3, \varepsilon_3) = (O((z_2 - \Omega)^4), 0, O((z_2 - \Omega)^4), O((z_2 - \Omega)^5)), \quad (3.59)$$

which converges to the origin as $z_2 \rightarrow \Omega$ (see Fig.10).

Let ρ_1 and ρ_3 be the small constants introduced in Sec.3.1 and Sec.3.3, respectively. Define Poincaré sections Σ_3^{in} and Σ_3^{out} to be

$$\Sigma_3^{in} = \{(\tilde{x}_3, r_3, z_3, \varepsilon_3) \mid |\tilde{x}_3| < \rho_1, 0 < r_3 \leq \rho_1, |z_3| \leq \rho_1, \varepsilon_3 = \rho_3\}, \quad (3.60)$$

$$\Sigma_3^{out} = \{(\tilde{x}_3, r_3, z_3, \varepsilon_3) \mid |\tilde{x}_3| < \rho_1, r_3 = \rho_1, |z_3| \leq \rho_1, 0 < \varepsilon_3 \leq \rho_3\}, \quad (3.61)$$

respectively (see Fig.10). Note that Σ_3^{in} is included in the section Σ_2^{out} (see Eq.(3.25)) if written in the K_2 coordinates and Σ_3^{out} in the section Σ_{out}^+ (see Eq.(3.6)) if written in the (X, Y, Z) coordinates.

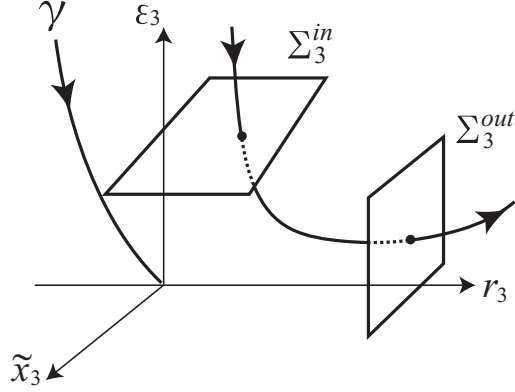


Fig. 10 Poincaré sections to define the transition map Π_3^{loc} .

Proposition 3.7. (I) If ρ_1 and ρ_3 are small, the transition map $\Pi_3^{loc} : \Sigma_3^{in} \rightarrow \Sigma_3^{out}$ along the flow of Eq.(3.58) is well-defined and expressed as

$$\Pi_3^{loc} \begin{pmatrix} \tilde{x}_3 \\ r_3 \\ z_3 \\ \rho_3 \end{pmatrix} = \begin{pmatrix} \beta_3(\rho_1) + r_3^4 \beta_4(\tilde{x}_3, r_3, z_3, \rho_3, \rho_1) \\ \rho_1 \\ \left(z_3 - \sqrt{6} \rho_3 + \rho_3 \beta_5(\tilde{x}_3, z_3, \rho_3) \right) \left(\frac{r_3}{\rho_1} \right)^4 + r_3^5 (\log r_3) \beta_6(\tilde{x}_3, r_3, z_3, \rho_3, \rho_1) \\ \rho_3 \left(\frac{r_3}{\rho_1} \right)^5 \end{pmatrix}, \quad (3.62)$$

where $\beta_3, \beta_4, \beta_5$ and β_6 are C^∞ functions with respect to \tilde{x}_3, z_3 and ρ_3 with the property that β_4 and β_6 are bounded as $r_3 \rightarrow 0$.

(II) As $r_3 \rightarrow 0$, $\Pi_3^{loc}(\tilde{x}_3, r_3, z_3, \rho_3)$ converges to the intersection point of Σ_3^{out} and the unstable manifold of the origin.

Before proving Prop.3.7, we need to derive the normal form of Eq.(3.58).

Lemma 3.8. In the vicinity of the origin, there exists a coordinate transformation

$$\begin{pmatrix} \tilde{x}_3 \\ r_3 \\ z_3 \\ \varepsilon_3 \end{pmatrix} = \Phi_1(X_3, r_3, Z_3, \varepsilon_3) := \begin{pmatrix} X_3 + \psi_3(X_3, Z_3, \varepsilon_3) \\ r_3 \\ Z_3 + \varepsilon_3 \psi_4(X_3, Z_3, \varepsilon_3) \\ \varepsilon_3 \end{pmatrix} \quad (3.63)$$

such that Eq.(3.58) is transformed into

$$\begin{cases} \dot{X}_3 = -3X_3 + \sqrt{\frac{3}{2}}Z_3 - c_1r_3 + r_3h_{33}(X_3, r_3, Z_3, \varepsilon_3), \\ \dot{r}_3 = \frac{1}{2}r_3, \\ \dot{Z}_3 = -2Z_3 - \sqrt{\frac{3}{2}}\varepsilon_3 + \varepsilon_3r_3h_{34}(X_3, r_3, Z_3, \varepsilon_3), \\ \dot{\varepsilon}_3 = -\frac{5}{2}\varepsilon_3, \end{cases} \quad (3.64)$$

where $\psi_4, h_{33}, h_{34} \sim O_p(1)$ and $\psi_3 \sim O_p(2)$ are C^∞ functions.

Proof of Lemma 3.8. When $r_3 = 0$, Eq.(3.58) is written as

$$\begin{cases} \dot{\tilde{x}}_3 = -3\tilde{x}_3 + \sqrt{\frac{3}{2}}z_3 + h_{30}(\tilde{x}_3, 0, z_3, \varepsilon_3), \\ \dot{z}_3 = -2z_3 - \sqrt{\frac{3}{2}}\varepsilon_3 + \varepsilon_3h_{31}(\tilde{x}_3, z_3, \varepsilon_3), \\ \dot{\varepsilon}_3 = -\frac{5}{2}\varepsilon_3. \end{cases} \quad (3.65)$$

Since eigenvalues of the Jacobian matrix at the origin of the right hand side of the above are $-3, -2, -5/2$ and satisfy the non-resonance condition, there exists a C^∞ transformation of the form $(\tilde{x}_3, z_3, \varepsilon_3) \mapsto (X_3 + \psi_3(X_3, Z_3, \varepsilon_3), Z_3 + \tilde{\psi}_4(X_3, Z_3, \varepsilon_3), \varepsilon_3)$ such that Eq.(3.65) is linearized (see Chow, Li and Wang [3]). The $\tilde{\psi}_4$ is of the form $\tilde{\psi}_4 = \varepsilon_3\psi_4$, where ψ_4 is a C^∞ function, because if $\varepsilon_3 = 0$, Eq.(3.65) gives $\dot{z}_3 = -2z_3$ and it follows that $Z_3 = z_3$ when $\varepsilon_3 = 0$. This transformation brings Eq.(3.58) into Eq.(3.64). \blacksquare

Proof of Prop.3.7 Note that even in the new coordinates $(X_3, r_3, Z_3, \varepsilon_3)$, the sections Σ_3^{in} and Σ_3^{out} are included in the hyperplanes $\{\varepsilon_3 = \rho_3\}$ and $\{r_3 = \rho_1\}$, respectively.

Let us calculate the transition time T from Σ_3^{in} to Σ_3^{out} . Since $r_3(t) = r_3(0)e^{t/2}$ and $\varepsilon_3(t) = \varepsilon_3(0)e^{-5t/2}$ from Eq.(3.64), T is given by

$$T = \log\left(\frac{\rho_1}{r_3(0)}\right)^2. \quad (3.66)$$

Further, by integrating the third equation of Eq.(3.64), $Z_3(t)$ is calculated as

$$Z_3(t) = Z_3(0)e^{-2t} + \sqrt{6}\rho_3(e^{-5t/2} - e^{-2t}) + e^{-2t} \int_0^t \rho_3 r_3(0) h_{34}(\mathbf{X}_3(s)) ds, \quad (3.67)$$

where $\mathbf{X}_3(s) = (X_3(s), r_3(s), Z_3(s), \varepsilon_3(s))$. Owing to the mean value theorem, there exists $0 \leq \tau = \tau(t) \leq t$ such that Eq.(3.67) is rewritten as

$$Z_3(t) = (Z_3(0) - \sqrt{6}\rho_3)e^{-2t} + \sqrt{6}\rho_3e^{-5t/2} + \rho_3r_3(0)e^{-2t}h_{34}(\mathbf{X}_3(\tau))t. \quad (3.68)$$

This and Eq.(3.66) are put together to yield

$$Z_3(T) = (Z_3(0) - \sqrt{6}\rho_3) \left(\frac{r_3(0)}{\rho_1} \right)^4 + \sqrt{6}\rho_3 \left(\frac{r_3(0)}{\rho_1} \right)^5 + \rho_3 \frac{r_3(0)^5}{\rho_1^4} h_{34}(\mathbf{X}_3(\tau(T)))T. \quad (3.69)$$

Before estimating $X_3(T)$, we prove (II) of Prop.3.7. To prove (II) of Prop.3.7, note that the hyperplane $\{r_3 = 0\}$ is invariant and included in the stable manifold of the origin. Since $(\tilde{x}_3, r_3, z_3, \rho_3)$ converges to the stable manifold as $r_3 \rightarrow 0$, $\Pi_3^{loc}(\tilde{x}_3, r_3, z_3, \rho_3)$ converges to the unstable manifold as $r_3 \rightarrow 0$ on account of the λ -lemma. This proves Prop.3.7 (II). Since the intersection of the unstable manifold and Σ_3^{out} depends only on ρ_1 , $X_3(T)$ is of the form

$$X_3(T) = h_{35}(\rho_1) + h_{36}(X_3(0), r_3(0), Z_3(0), \rho_3, \rho_1), \quad (3.70)$$

where h_{35} is a C^∞ functions such that $h_{35}(\rho_1)$ gives the X_3 component of the intersection point and where h_{36} is a C^∞ function with respect to $X_3(0), Z_3(0)$ and ρ_3 such that $h_{36} \rightarrow 0$ as $r_3(0) \rightarrow 0$. By using linearized equation of Eq.(3.64), it is easy to verify that h_{36} decays as $h_{36} \sim O(r_3(0)^4)$. Thus the transition map $\tilde{\Pi}_3^{loc}$ from Σ_3^{in} to Σ_3^{out} along the flow of Eq.(3.64) is given by

$$\tilde{\Pi}_3^{loc} \begin{pmatrix} X_3 \\ r_3 \\ Z_3 \\ \rho_3 \end{pmatrix} = \begin{pmatrix} h_{35}(\rho_1) + r_3^4 h_{37}(X_3, r_3, Z_3, \rho_3, \rho_1) \\ (Z_3 - \sqrt{6}\rho_3) \left(\frac{r_3}{\rho_1} \right)^4 + \sqrt{6}\rho_3 \left(\frac{r_3}{\rho_1} \right)^5 - 2\rho_3 \frac{r_3^5}{\rho_1^4} \log \left(\frac{r_3}{\rho_1} \right) h_{38}(X_3, r_3, Z_3, \rho_3, \rho_1) \\ \rho_3 \left(\frac{r_3}{\rho_1} \right)^5 \end{pmatrix}, \quad (3.71)$$

where h_{37} is bounded as $r_3 \rightarrow 0$, and where $h_{38}(X_3, r_3, Z_3, \rho_3, \rho_1) = h_{34}(\mathbf{X}_3(\tau(T)))$ is bounded as $r_3(0) \rightarrow 0$ because a solution $\mathbf{X}_3(t)$ of Eq.(3.64) is bounded as $r_3(0) \rightarrow 0$ for $0 \leq t \leq T$. Now Eq.(3.62) is verified by calculating $\Phi_1 \circ \tilde{\Pi}_3^{loc} \circ \Phi_1^{-1}$. Note that β_5 in Eq.(3.62) is independent of r_3 and ρ_1 because it is the inverse of the transformation (3.63). This proves Prop.3.7 (I). \blacksquare

3.6 Proof of Theorem 3.2

We are now in a position to prove Theorem 3.2. Let $\tau_x : (x, r, z, \varepsilon) \mapsto (x - \sqrt{2/3}, r, z, \varepsilon)$ be the translation in the x direction introduced in Sec.3.5. Eq.(3.7) is obtained by writing out the map $\tilde{\Pi}_{loc}^+ := \tau_x \circ \Pi_3^{loc} \circ \tau_x^{-1} \circ \kappa_{23} \circ \Pi_2^{loc} \circ \kappa_{12} \circ \Pi_1^{loc}$ and blowing it down to the (X, Y, Z)

coordinates. At first, $\Pi_2^{loc} \circ \kappa_{12} \circ \Pi_1^{loc}$ is calculated as

$$\begin{aligned} & \begin{pmatrix} x_1 \\ y_1 \\ \rho_1 \\ \varepsilon_1 \end{pmatrix} \xrightarrow{\Pi_1^{loc}} \begin{pmatrix} \varphi_1 + \tilde{X}_1(1 + \beta_1) \\ \varphi_2 + \tilde{Y}_1(1 + \beta_2) \\ \rho_1 \varepsilon_1^{1/5} \rho_2^{-1/5} \\ \rho_2 \end{pmatrix} \xrightarrow{\kappa_{12}} \begin{pmatrix} \rho_2^{-3/5} \varphi_1 + \rho_2^{-3/5} \tilde{X}_1(1 + \beta_1) \\ \rho_2^{-2/5} \varphi_2 + \rho_2^{-2/5} \tilde{Y}_1(1 + \beta_2) \\ \rho_2^{-4/5} \\ \rho_1 \varepsilon_1^{1/5} \end{pmatrix} \\ & \xrightarrow{\Pi_2^{loc}} \begin{pmatrix} p_x + H_1(\rho_2^{-3/5} \varphi_1 + \rho_2^{-3/5} \tilde{X}_1(1 + \beta_1) - q_x, \rho_2^{-2/5} \varphi_2 + \rho_2^{-2/5} \tilde{Y}_1(1 + \beta_2) - q_y, \rho_1 \varepsilon_1^{1/5}, \rho_3) \\ \rho_3^{-2/5} \\ p_z + H_2(\rho_2^{-3/5} \varphi_1 + \rho_2^{-3/5} \tilde{X}_1(1 + \beta_1) - q_x, \rho_2^{-2/5} \varphi_2 + \rho_2^{-2/5} \tilde{Y}_1(1 + \beta_2) - q_y, \rho_1 \varepsilon_1^{1/5}, \rho_3) \\ \rho_1 \varepsilon_1^{1/5} \end{pmatrix}, \end{aligned} \quad (3.72)$$

where $\varphi_1 = \varphi_1(\rho_1 \varepsilon_1^{1/5} \rho_2^{-1/5}, \rho_2)$, $\varphi_2 = \varphi_2(\rho_1 \varepsilon_1^{1/5} \rho_2^{-1/5}, \rho_2)$ and \tilde{X}_1, \tilde{Y}_1 are defined by Eqs.(3.48, 44), respectively. In what follows, we omit the arguments of H_1 and H_2 . The last term in the above is further mapped to

$$\xrightarrow{\kappa_{23}} \begin{pmatrix} \rho_3^{3/5} p_x + \rho_3^{3/5} H_1 \\ \rho_1 \rho_3^{-1/5} \varepsilon_1^{1/5} \\ \rho_3^{4/5} p_z + \rho_3^{4/5} H_2 \\ \rho_3 \end{pmatrix} \xrightarrow{\tau_x^{-1}} \begin{pmatrix} \sqrt{2/3} + \rho_3^{3/5} p_x + \rho_3^{3/5} H_1 \\ \rho_1 \rho_3^{-1/5} \varepsilon_1^{1/5} \\ \rho_3^{4/5} p_z + \rho_3^{4/5} H_2 \\ \rho_3 \end{pmatrix} := \begin{pmatrix} \tilde{x}_3 \\ r_3 \\ z_3 \\ \rho_3 \end{pmatrix}. \quad (3.73)$$

Let us denote the resultant as $(\tilde{x}_3, r_3, z_3, \rho_3)$ as above. Then, $\tilde{\Pi}_{loc}^+$ proves to be given by

$$\begin{aligned} \tilde{\Pi}_{loc}^+ \begin{pmatrix} x_1 \\ y_1 \\ \rho_1 \\ \varepsilon_1 \end{pmatrix} &= \begin{pmatrix} -\sqrt{2/3} + \beta_3(\rho_1) + r_3^4 \beta_4(\tilde{x}_3, r_3, z_3, \rho_3, \rho_1) \\ \rho_1 \\ (z_3 - \sqrt{6}\rho_3 + \rho_3 \beta_5(\tilde{x}_3, z_3, \rho_3)) \left(\frac{r_3}{\rho_1}\right)^4 + r_3^5 (\log r_3) \beta_6(\tilde{x}_3, r_3, z_3, \rho_3, \rho_1) \\ \rho_3 \left(\frac{r_3}{\rho_1}\right)^5 \end{pmatrix} \\ &= \begin{pmatrix} -\sqrt{2/3} + \beta_3(\rho_1) + \rho_1^4 \rho_3^{-4/5} \varepsilon_1^{4/5} \beta_4(\tilde{x}_3, \rho_1 \rho_3^{-1/5} \varepsilon_1^{1/5}, z_3, \rho_3, \rho_1) \\ \rho_1 \\ (z_3 - \sqrt{6}\rho_3 + \rho_3 \beta_5(\tilde{x}_3, z_3, \rho_3)) \left(\frac{\varepsilon_1}{\rho_3}\right)^{4/5} + O(\varepsilon_1 \log \varepsilon_1) \\ \varepsilon_1 \end{pmatrix}. \end{aligned} \quad (3.74)$$

The third component of the above is calculated as

$$\begin{aligned} & (z_3 - \sqrt{6}\rho_3 + \rho_3 \beta_5(\tilde{x}_3, z_3, \rho_3)) \left(\frac{\varepsilon_1}{\rho_3}\right)^{4/5} + O(\varepsilon_1 \log \varepsilon_1) \\ &= \left(\Omega + O(\rho_3) + H_2(\hat{X}, \hat{Y}, \rho_1 \varepsilon_1^{1/5}, \rho_3) + \rho_3^{1/5} \beta_5(\tilde{x}_3, z_3, \rho_3)\right) \varepsilon_1^{4/5} + O(\varepsilon_1 \log \varepsilon_1), \end{aligned} \quad (3.75)$$

where

$$\hat{X} = \rho_2^{-3/5} \varphi_1 + \rho_2^{-3/5} \tilde{X}_1(1 + \beta_1) - q_x, \quad \hat{Y} = \rho_2^{-2/5} \varphi_1 + \rho_2^{-2/5} \tilde{Y}_1(1 + \beta_2) - q_y.$$

From Eq.(3.29), Eq.(3.75) is rewritten as

$$\left(\Omega + O(\rho_3) + \tilde{H}_2(\hat{X}, \hat{Y}, \rho_3) + \rho_3^{1/5} \beta_5(\tilde{x}_3, z_3, \rho_3) \right) \varepsilon_1^{4/5} + O(\varepsilon_1 \log \varepsilon_1). \quad (3.76)$$

Since \tilde{H}_2 and $\rho_3^{1/5} \beta_5(\tilde{x}_3, z_3, \rho_3)$ are C^1 with respect to $\rho_3^{1/5}$ (see Eq.(3.39)) and since $\tilde{\Pi}_{loc}^+(x_1, y_1, \rho_1, \varepsilon_1)$ is independent of ρ_3 which is introduced to define the intermediate sections Σ_2^{out} and Σ_3^{in} , Eq.(3.76) has to be of the form

$$\left(\Omega + \hat{H}_2(\hat{X}, \hat{Y}) \right) \varepsilon_1^{4/5} + O(\varepsilon_1 \log \varepsilon_1). \quad (3.77)$$

Now we look into \hat{X} and \hat{Y} . Since $\varphi_1(x_1, \varepsilon_1)$ and $\varphi_2(y_1, \varepsilon_1)$ give the graph of the center manifold W^c , $x_1 = \varphi_1(0, \varepsilon_1)$ and $y_1 = \varphi_2(0, \varepsilon_1)$ coincide with the orbit γ of the first Painlevé equation written in the K_1 coordinates. Thus we obtain

$$\begin{aligned} \hat{X} &= \rho_2^{-3/5} \varphi_1(\rho_1 \varepsilon_1^{1/5} \rho_2^{-1/5}, \rho_2) + \rho_2^{-3/5} \tilde{X}_1(1 + \beta_1) - q_x \\ &= \left(\rho_2^{-3/5} \varphi_1(0, \rho_2) - q_x \right) + \rho_2^{-3/5} \tilde{X}_1(1 + \beta_1) + O((\varepsilon_1/\rho_2)^{1/5}) \\ &= \rho_2^{-3/5} (D_1 x_1 + D_2 y_1) \left(\frac{\rho_2}{\varepsilon_1} \right)^{3/5} \exp\left[-\frac{dc_1 \rho_1}{\varepsilon_1} \right] \left(1 + O((\varepsilon_1/\rho_2)^{1/5}) \right) + O((\varepsilon_1/\rho_2)^{1/5}) \\ &= (D_1 x_1 + D_2 y_1) \varepsilon_1^{-3/5} \exp\left[-\frac{dc_1 \rho_1}{\varepsilon_1} \right] \left(1 + O((\varepsilon_1/\rho_2)^{1/5}) \right) + O((\varepsilon_1/\rho_2)^{1/5}). \end{aligned} \quad (3.78)$$

The \hat{Y} is calculated in the same manner. Further, since Eq.(3.77) is independent of ρ_2 which is introduced to define the intermediate sections Σ_1^{out} and Σ_2^{in} , Eq.(3.77) is rewritten as

$$\left(\Omega + \hat{H}_2\left((D_1 x_1 + D_2 y_1) \varepsilon_1^{-3/5} \exp\left[-\frac{dc_1 \rho_1}{\varepsilon_1} \right], (D_3 x_1 + D_4 y_1) \varepsilon_1^{-2/5} \exp\left[-\frac{dc_1 \rho_1}{\varepsilon_1} \right] \right) \right) \varepsilon_1^{4/5} + O(\varepsilon_1 \log \varepsilon_1). \quad (3.79)$$

Our final task is to blow down Eq.(3.74) with Eq.(3.79) to the (X, Y, Z) coordinates to obtain Eq.(3.7). Theorem 3.2 (II) follows from Prop.3.3, Prop.3.6 (II), Prop.3.7 (II) and the fact that the unstable manifold described in Prop.3.7 (II) coincides with the heteroclinic orbit α^+ if written in the (X, Y, Z) coordinates. Theorem 3.2 (III) follows from Lemma 3.4. This complete the proof of Theorem 3.2 ■

4 Global analysis and the proof of main theorems

In this section, we construct a global Poincaré map by combining a succession of transition maps (see Fig.4) and prove Theorems 1 and 2.

4.1 Global Poincaré map

In what follows, we suppose that the system (1.5) admits a \mathbf{Z}_2 symmetry such that $S_a^+ \cup \{L^+\}$ and $S_a^- \cup \{L^-\}$ are exchanged to each other as Eq.(2.5) does. It facilitates our calculation, since the global Poincaré map reduced to the composition of the transition maps from Σ_{out}^- to Σ_{out}^+ (see Fig. 4), where Σ_{out}^- corresponds to Σ_{out}^+ by the \mathbf{Z}_2 symmetry. The proof of Theorems 1 and 2 without this assumption can be done in a similar way.

Recall that (X, Y, Z) coordinates are defined near the fold point L^+ and that the sections Σ_{in}^+ and Σ_{out}^+ are defined in Eq.(3.6). Take the new section

$$\Sigma_I^+ = \{Z = \rho_1^4 + e^{-1/\varepsilon^2}\} \quad (4.1)$$

and change the coordinates so that in a region above Σ_I^+ , S_a^+ is expressed as

$$\{(X, Y, Z) \in S_a^+ \mid Z \geq \rho_1^4 + e^{-1/\varepsilon^2}\} = \{X = 0, Y = -\eta, Z \geq \rho_1^4 + e^{-1/\varepsilon^2}\}, \quad (4.2)$$

with some positive constant η . We can define such coordinates without changing the expression of Π_{loc}^+ given in Eq.(3.7) by using a partition of unity. We can change the coordinates near $S_a^- \cup \{L^-\}$ in a similar manner without changing the coordinate expression near $S_a^+ \cup \{L^+\}$ (see Fig.11). Let

$$\begin{cases} \dot{X} = \tilde{f}_1(X, Y, Z, \varepsilon, \delta), \\ \dot{Y} = \tilde{f}_2(X, Y, Z, \varepsilon, \delta), \\ \dot{Z} = \varepsilon \tilde{g}(X, Y, Z, \varepsilon, \delta), \end{cases} \quad (4.3)$$

be the system (1.5) written in the resultant coordinates.

Let U_{out}^- be a small neighborhood of the point $\alpha^- \cap \Sigma_{out}^-$ and let $(X_0, Y_0, Z_0) \in U_{out}^- \cap \Sigma_{out}^-$. By using the boundary layer theory, we can show that the solution of Eq.(4.3) whose initial value is (X_0, Y_0, Z_0) is given as

$$\begin{cases} X(t) = P_x(t; X_0, Y_0, Z_0) + O(\varepsilon), \\ Y(t) = -\eta + P_y(t; X_0, Y_0, Z_0) + O(\varepsilon), \\ Z(t) = Z_0 + O(\varepsilon t), \end{cases} \quad (4.4)$$

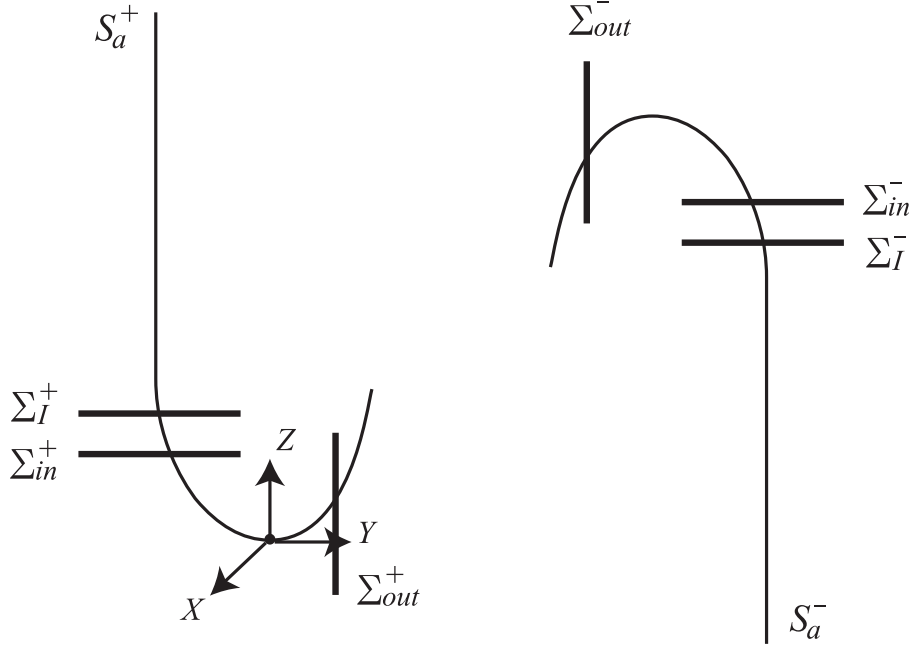


Fig. 11 Coordinate for calculating the global Poincaré map.

if $0 \leq t \leq 1/\varepsilon$, where $P_x(t; X_0, Y_0, Z_0)$ and $P_y(t; X_0, Y_0, Z_0)$ are solutions of the system

$$\dot{X} = \tilde{f}_1(X, -\eta + Y, Z_0, 0, \delta), \quad \dot{Y} = \tilde{f}_2(X, -\eta + Y, Z_0, 0, \delta), \quad (4.5)$$

(see O'Mally [15]). Since the unperturbed system has the solution α^- which converges to S_a^+ , solutions of Eq.(4.3) passing near the α^- approach S_a^+ , and both P_x and P_y tend to zero as $t \rightarrow \infty$.

Note that Eq.(4.5) corresponds to Eq.(2.4) if $Z_0 = z_0^-$, the Z component of L^- . Because of the assumption (A6), there exists an open neighborhood V^+ of $(X, Y) = (0, -\eta)$, which is independent of δ , such that solutions of Eq.(4.5) whose initial values are in V^+ converge to $(0, -\eta)$ exponentially. Let $\tilde{V}^+ = V^+ \times S_a^+$ and define the section Σ_{II}^+ to be

$$\Sigma_{II}^+ = \tilde{V}^+ \cap \{(X, Y, Z) \mid X = 0, |Z - z_0^-| \leq \rho_4\}, \quad (4.6)$$

where ρ_4 is a small positive number so that the solution of Eq.(4.3) through (X_0, Y_0, Z_0) intersects Σ_{II}^+ only once (see Fig.12).

The transition map $\Pi_{out,II}^+$ from Σ_{out}^- to Σ_{II}^+ is given by

$$\Pi_{out,II}^+ \begin{pmatrix} X \\ Y \\ Z \end{pmatrix} = \begin{pmatrix} P_x(T; X, Y, Z) + O(\varepsilon) \\ -\eta + P_y(T; X, Y, Z) + O(\varepsilon) \\ Z + O(\varepsilon) \end{pmatrix}, \quad (4.7)$$

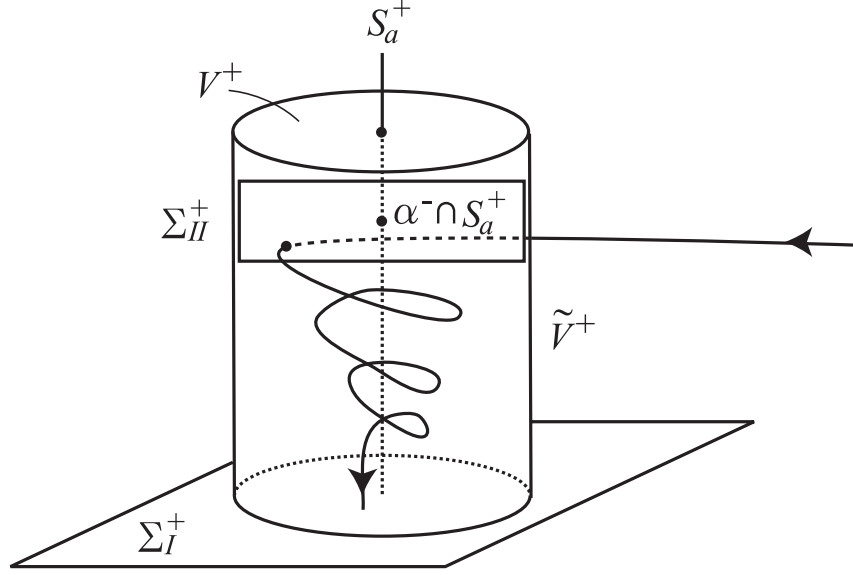


Fig. 12 The section Σ_{II}^+ and an orbit of Eq.(4.3).

where $T = T(X, Y, Z, \delta)$ is the transition time. Since V^+ is independent of δ , there exist positive numbers M and m , which are also independent of δ , such that $m \leq T(X, Y, Z, \delta) \leq M$ for any $\delta > 0$. Thus $T \sim O(1)$ as $\varepsilon \rightarrow 0$ and $\delta \rightarrow 0$ (remember that to prove Thm.2, we suppose that $\delta = \delta(\varepsilon)$ is also small as well as ε).

Next thing to do is to construct a transition map $\Pi_{II,I}^+$ from Σ_{II}^+ to Σ_I^+ . Because of the assumption (A5), there exists an affine transformation $(X, Y) \mapsto (\xi_1, \xi_2)$ such that Eq.(4.5) is brought into the form

$$\frac{d}{dt} \begin{pmatrix} \xi_1 \\ \xi_2 \end{pmatrix} = \sqrt{-1}\omega^+(Z_0, \delta) \begin{pmatrix} 1 & 0 \\ 0 & -1 \end{pmatrix} \begin{pmatrix} \xi_1 \\ \xi_2 \end{pmatrix} - \delta\mu^+(Z_0, \delta) \begin{pmatrix} 1 & 0 \\ 0 & 1 \end{pmatrix} \begin{pmatrix} \xi_1 \\ \xi_2 \end{pmatrix} + f_3(\xi_1, \xi_2, Z_0, \delta), \quad (4.8)$$

where f_3 is the higher order term with respect to ξ_1 and ξ_2 . We transform Eq.(4.8) into the normal form with respect to the first term in the right hand side as we did for Eq.(2.6). There exists a transformation of the form

$$\xi_1 = re^{i\theta} + O(r^2), \quad \xi_2 = re^{-i\theta} + O(r^2), \quad (4.9)$$

such that Eq.(4.8) is rewritten as

$$\begin{cases} \dot{r} = -\delta\mu^+(Z_0, \delta)r + O(r^3), \\ \dot{\theta} = \omega^+(Z_0, \delta) + O(r^2). \end{cases} \quad (4.10)$$

Since solutions in V^+ decay as $O(\exp[-\delta\mu^+(Z_0, \delta)t])$ and since solutions are well approximated by solutions of the linearized equation of Eq.(4.10) if t is large, a solution of Eq.(4.10) whose initial value is (r_0, θ_0) is written as

$$\begin{cases} r(t) = K_1(r_0, \theta_0, Z_0, \delta) (1 + K_2(t; r_0, \theta_0, Z_0, \delta)) e^{-\delta\mu^+(Z_0, \delta)t}, \\ \theta(t) = \omega^+(Z_0, \delta)t (1 + K_3(t; r_0, \theta_0, Z_0, \delta)) + \theta_0, \end{cases} \quad (4.11)$$

where K_1, K_2 and K_3 are C^∞ functions with respect to r_0, θ_0, Z_0 and δ such that K_2 and K_3 are exponentially small if t is large. From Eq.(4.11) together with the fact that the transition time from Σ_{II}^+ to Σ_I^+ is of order $O(1/\varepsilon)$, $\Pi_{II,I}^+$ turns out to take the form

$$\begin{aligned} & \Pi_{II,I}^+ \begin{pmatrix} X \\ Y \\ Z \end{pmatrix} \\ &= \begin{pmatrix} \left(K_4(X, Y, Z, \delta) \sin\left(\frac{\omega^+(Z, \delta)}{\varepsilon}\right) + K_5(X, Y, Z, \delta) \cos\left(\frac{\omega^+(Z, \delta)}{\varepsilon}\right) \right) e^{-\delta\mu^+(Z, \delta)/\varepsilon} (1 + K_8(X, Y, Z, \delta, \varepsilon)) \\ -\eta + \left(K_6(X, Y, Z, \delta) \sin\left(\frac{\omega^+(Z, \delta)}{\varepsilon}\right) + K_7(X, Y, Z, \delta) \cos\left(\frac{\omega^+(Z, \delta)}{\varepsilon}\right) \right) e^{-\delta\mu^+(Z, \delta)/\varepsilon} (1 + K_9(X, Y, Z, \delta, \varepsilon)) \\ \rho_1^4 + e^{-1/\varepsilon^2} \end{pmatrix}, \end{aligned} \quad (4.12)$$

where K_i ($i = 4, \dots, 9$) are C^∞ functions with respect to X, Y, Z and δ such that K_8 and K_9 are exponentially smaller than 1.

Since the transition map $\Pi_{I,in}^+$ from Σ_I^+ to Σ_{in}^+ is exponentially close to the identity map, the transition map from Σ_{out}^- to Σ_{in}^+ is given by

$$\begin{aligned} & \Pi_{I,in}^+ \circ \Pi_{II,I}^+ \circ \Pi_{out,II}^+ \begin{pmatrix} X \\ Y \\ Z \end{pmatrix} \\ &= \begin{pmatrix} \left(K_{10}(X, Y, Z, \delta) \sin\left(\frac{\omega^+(Z, \delta)}{\varepsilon}\right) + K_{11}(X, Y, Z, \delta) \cos\left(\frac{\omega^+(Z, \delta)}{\varepsilon}\right) \right) e^{-\delta\mu^+(Z, \delta)/\varepsilon} (1 + O(\varepsilon)) \\ -\eta + \left(K_{12}(X, Y, Z, \delta) \sin\left(\frac{\omega^+(Z, \delta)}{\varepsilon}\right) + K_{13}(X, Y, Z, \delta) \cos\left(\frac{\omega^+(Z, \delta)}{\varepsilon}\right) \right) e^{-\delta\mu^+(Z, \delta)/\varepsilon} (1 + O(\varepsilon)) \\ \rho_1^4 \end{pmatrix}, \end{aligned} \quad (4.13)$$

where K_i ($i = 10, \dots, 13$) are C^∞ functions with respect to X, Y, Z and δ . Finally, the transition map Π^+ from Σ_{out}^- to Σ_{out}^+ will be obtained by composing the above $\Pi_{I,in}^+ \circ \Pi_{II,I}^+ \circ \Pi_{out,II}^+$ and Π_{loc}^+ given in Eq.(3.7). The global Poincaré map Π is given by $\Pi = \Pi^+ \circ \Pi^+$ because of the \mathbf{Z}_2 symmetry. The remaining task is now to investigate Π^+ .

4.2 Derivative of the transition map

Let us identify two sections Σ_{out}^- and Σ_{out}^+ by the \mathbf{Z}_2 symmetry and regard Π^+ as the map from an open subset of Σ_{out}^+ into itself.

Simple calculation shows that the derivative of Π^+ with respect to (X, Z) is expressed as

$$e^{-\delta\mu^+(Z,\delta)/\varepsilon} e^{-dc_1\rho_1/\varepsilon} \begin{pmatrix} k_1\varepsilon^{4/5} & k_2\varepsilon^{-1/5} \\ k_3\varepsilon^{1/5} & k_4\varepsilon^{-4/5} \end{pmatrix} + \text{h.o.t.}, \quad (4.14)$$

where $k_i = k_i(X, Y, Z, \delta)$ ($i = 1, \dots, 4$) are C^∞ functions which are nonzero as $\delta \rightarrow 0$ and where h.o.t. (higher order term) denotes infinitesimally smaller terms than the first term as $\varepsilon \rightarrow 0$. Recall that the constant c_1 appears in Eq.(3.1). Since Eq.(3.1) satisfies the assumption (A5), it is easy to verify that $c_1 \sim O(\delta\mu^+(Z, \delta))$ by estimating eigenvalues of the Jacobian matrix on S_a^+ of the right hand side of Eq.(3.1). Thus the eigenvalues λ_\pm of Eq.(4.14) are estimated as

$$\lambda_+ \sim O(e^{-c_2\delta/\varepsilon} \varepsilon^{-4/5}), \quad \lambda_- \sim O(e^{-c_2\delta/\varepsilon} \varepsilon^{4/5}), \quad (4.15)$$

respectively, where c_2 is some positive constant.

4.3 Proof of Theorems 1 and 2

Now we are in a position to prove Theorems 1 and 2.

Proof of Thm.1. Since δ is fixed in this theorem, we can suppose that Eq.(1.5) is independent of δ and the assumptions (A5) and (A6) are automatically satisfied. Thus the map (4.13) is valid and it is easy to verify that the transition map Π^+ from Σ_{out}^- to Σ_{out}^+ is contractive and eigenvalues λ_\pm are exponentially small if $\varepsilon > 0$ is small. It then turns out that Π^+ has a hyperbolically stable fixed point. ■

Proof of Thm.2. Now we suppose that $\delta = \delta(\varepsilon)$ is also small. Note that the analysis based on perturbation techniques with respect to ε is still valid as long as $\delta(\varepsilon) \gg \varepsilon$. We will prove the existence of a horseshoe.

Take a rectangle R on Σ_{out}^- whose edges are parallel to the X axis and the Z axis (see Fig.4). Let $h_R \sim O(\varepsilon)$ be the height of R . The image of R under the transition map $\Pi_{out,II}^+$ is a deformed rectangle whose ‘‘height’’ is also of order $O(\varepsilon)$, since the transition time from Σ_{out}^- to Σ_{II}^+ is of order $O(1)$ and $\dot{Z} \sim O(\varepsilon)$.

Next thing to consider is the shape of $\Pi_{II,I}^+ \circ \Pi_{out,II}^+(R)$. It is easy to show by using Eq.(4.11) that the image of $\Pi_{out,II}^+(R)$ under the map $\Pi_{II,I}^+$ becomes a ring-shaped area whose radius is of order $O(e^{-\delta\mu^+(Z_0,\delta)/\varepsilon})$. Since the transition time $t = t(Z)$ from the point $(X, Y, Z) \in \Sigma_{II}^+$ to Σ_I^+ is roughly estimated as $t(Z) \sim Z/\varepsilon$, the rotation angle of the ring-shaped area is estimated as

$$\omega^+(Z_0 + h_R, \delta) \cdot t(Z_0 + h_R) - \omega^+(Z_0, \delta) \cdot t(Z_0) \sim O(h_R/\varepsilon) \sim O(1). \quad (4.16)$$

Thus we can choose $h_R \sim O(\varepsilon)$ so that the rotation angle of the ring-shaped area is sufficiently close to 2π as is shown in Fig.13.

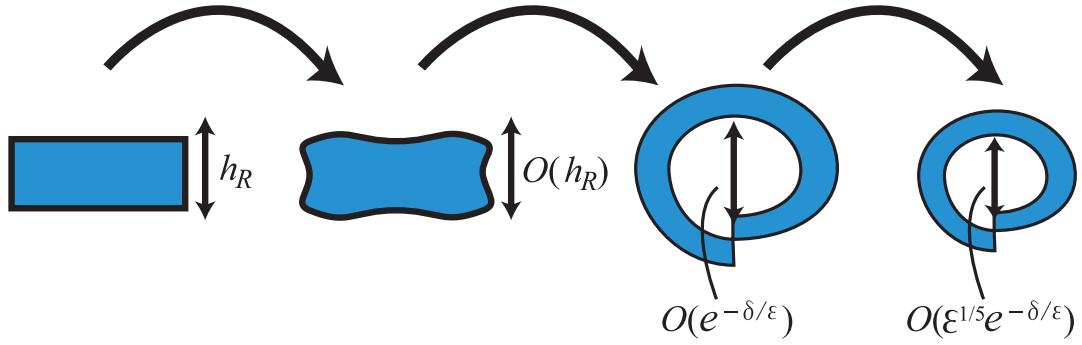


Fig. 13 Images of the rectangle R under a succession of transition maps.

Finally, we consider the shape of $\Pi^+(R)$ by using Eq.(3.7). Since

$$H(X, Y)\varepsilon^{4/5} \sim (D_1X + D_2Y)\varepsilon^{1/5} \exp[-dc_1\rho_1/\varepsilon] \quad (4.17)$$

holds by virtue of Eq.(3.9), if X and Y are small and since $c_1 \sim O(\delta)$, the radius of $\Pi^+(R)$ is of order $O(\varepsilon^{1/5} e^{-c_3\delta/\varepsilon})$ with some positive constant c_3 . If we put $\delta = \varepsilon(-\log \varepsilon)^{1/2}$, then the inequality

$$h_R \sim O(\varepsilon) \ll O(\varepsilon^{1/5} e^{-c_3\delta/\varepsilon}) \quad (4.18)$$

holds, which implies that Π^+ has a horseshoe as in Fig.5 (b) (recall that Π^+ is regarded as the map from Σ_{out}^+ into itself and there exists a ‘‘copy’’ of R on Σ_{out}^+). Hyperbolicity is easily proved because in this case, $|\lambda_+| \gg 1$ while $|\lambda_-| \ll 1$. This proves Theorem 2. ■

5 Concluding remarks

Our assumption for codimension 2 fold points is not generic in the sense that the Jacobian matrix has two zero eigenvalues. However, this assumption is not essential for existence of periodic orbits or chaotic invariant sets.

At first, we remark that Theorems 1 and 2 hold even if we add a small perturbation to Eq.(1.5), since hyperbolic invariant sets remain to exist under small perturbations.

We can consider the case that one of the connected components of critical manifolds consists of a codimension 1 fold point (*i.e.* a saddle-node bifurcation point of a unperturbed system), stable nodes, and stable focuses as in Fig.14. In this case, Theorem 1 is proved in a similar way and Theorem 2 still holds if the length of the subset of the critical manifold consisting of stable focuses is of order $O(1)$. Analysis of codimension 1 fold points is well performed in [7,8,11,12,13] and we do not deal with such a situation in this paper.

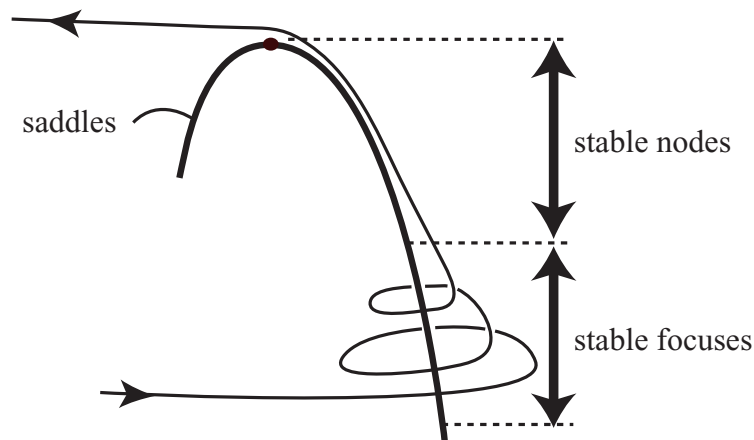


Fig. 14 Critical manifold consisting of a codimension 1 fold point, stable nodes, and stable focuses and an orbit near it.

We can also consider the case that one of the connected components \tilde{S} of critical manifolds has no fold points but consists of saddles with heteroclinic orbits α^\pm , see Fig.15. In this case, analysis around the \tilde{S} is done by using the exchange lemma (see Jones [10]) and we can prove theorems similar to Theorems 1 and 2.

Reference

- [1] W. Balser, Formal power series and linear systems of meromorphic ordinary differential equations, Springer-Verlag, New York, (2000)
- [2] H. Chiba, C^1 approximation of vector fields based on the renormalization group method, SIAM j. on Appl. dyn. syst. Vol.7 (2008), no.3, 895–932
- [3] S. N. Chow, C. Li, D. Wang, Normal forms and bifurcation of planar vector fields, Cambridge University Press, Cambridge, (1994)
- [4] F. Dumortier, Singularities of vector fields on the plane, J.Differential Equations 23

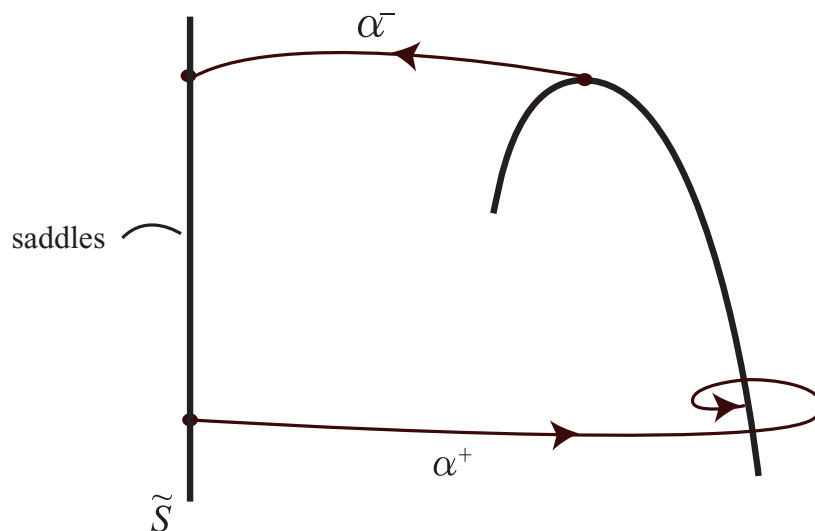


Fig. 15 Two connected components of critical manifolds. One is similar to that of our system (1.5) and the other consists of only saddles.

(1977), no. 1, 53–106

- [5] F. Dumortier, R. Roussarie, Canard cycles and center manifolds, *Mem. Amer. Math. Soc.* 121 (1996), no. 577
- [6] N. Fenichel, Geometric singular perturbation theory for ordinary differential equations, *J. Differential Equations* 31 (1979), no. 1, 53–98
- [7] S. van Gils, M. Krupa, P. Szmolyan, Asymptotic expansions using blow-up, *Z. Angew. Math. Phys.* 56 (2005), no. 3, 369–397
- [8] J. Guckenheimer, M. Wechselberger, L.S. Young, Chaotic attractors of relaxation oscillators, *Nonlinearity* 19 (2006), no. 3, 701–720
- [9] E. L. Ince, *Ordinary Differential Equations*, Dover Publications, New York, (1944)
- [10] C. K. R. T. Jones, Geometric singular perturbation theory, *Dynamical systems (Montecatini Terme, 1994)*, 44–118, *Lecture Notes in Math.*, 1609, Springer, Berlin, 1995
- [11] M. Krupa, P. Szmolyan, Extending geometric singular perturbation theory to nonhyperbolic points —fold and canard points in two dimensions, *SIAM J. Math. Anal.* 33 (2001), no. 2, 286–314
- [12] M. Krupa, P. Szmolyan, Extending slow manifolds near transcritical and pitchfork singularities, *Nonlinearity* 14 (2001), no. 6, 1473–1491
- [13] E. Mischenko, N. Rozov, *Differential Equations with Small Parameters and Relaxation*

- Oscillations, Plenum Press New York, (1980)
- [14] V. A. Noonburg, A separating surface for the Painleve differential equation $x'' = x^2 - t$, J. Math. Anal. Appl. 193 (1995), no. 3, 817–831
 - [15] R.E. O'Mally Jr., Introduction to Singular Perturbation, Academic Press, New York, (1974)
 - [16] L. P. Silnikov, A case of the existence of a denumerable set of periodic motions, Dokl. Akad. Nauk SSSR 160 (1965) 558-561
 - [17] P. Szmolyan, M. Wechselberger, Canards in \mathbf{R}^3 , J. Differential Equations 177 (2001), no. 2, 419–453
 - [18] P. Szmolyan, M. Wechselberger, Relaxation oscillations in \mathbf{R}^3 , J. Differential Equations 200 (2004), no. 1, 69–104
 - [19] S. Wiggins, Global bifurcations and chaos, Springer-Verlag, New York, (1988)
 - [20] A.J. Homburg, Ale Jan Periodic attractors, strange attractors and hyperbolic dynamics near homoclinic orbits to saddle-focus equilibria, Nonlinearity 15 (2002), no.4, 1029–1050